
AFRL-RW-EG-TR-2012-009

# Benchtop Energetics: Research Progress, Concept Evaluation, and Apparatus Development

Mario E. Fajardo
William K. Lewis III
Voncile L. Ashley
Rachel M. Nep
Emily C. Fossum
Christopher D. Molek

Air Force Research Laboratory
Munitions Directorate/Ordnance Division
Energetic Materials Branch (AFRL/RWME)
Eglin AFB, FL 32542-5910

31 January 2012

Final Report



AIR FORCE RESEARCH LABORATORY, MUNITIONS DIRECTORATE
Air Force Materiel Command ■ United States Air Force ■ Eglin Air Force Base

## NOTICE AND SIGNATURE PAGE

Using Government drawings, specifications, or other data included in this document for any purpose other than Government procurement does not in any way obligate the U.S. Government. The fact that the Government formulated or supplied the drawings, specifications, or other data does not license the holder or any other person or corporation; or convey any rights or permission to manufacture, use, or sell any patented invention that may relate to them.

Qualified requestors may obtain copies of this report from the Defense Technical Information Center (DTIC) (http://www.dtic.mil).

AFRL-RW-EG-TR-2012-009 HAS BEEN REVIEWED AND IS APPROVED FOR PUBLICATION IN ACCORDANCE WITH ASSIGNED DISTRIBUTION STATEMENT.

FOR THE DIRECTOR:

| | | |
|---|---|---|
| //ORIGINAL SIGNED// | //ORIGINAL SIGNED// | //ORIGINAL SIGNED// |
| HOWARD G. WHITE, PhD | JENNIFER L. JORDAN, PhD | MARIO E. FAJARDO, PhD |
| Technical Advisor | Technical Advisor | Project Manager |
| Ordnance Division | Energetic Materials Branch | Energetic Materials Branch |

This report is published in the interest of scientific and technical information exchange, and its publication does not constitute the Government's approval or disapproval of its ideas or findings.

This page intentionally left blank

# REPORT DOCUMENTATION PAGE

*Form Approved*
*OMB No. 0704-0188*



| **1. REPORT DATE** *(DD-MM-YYYY)* | **2. REPORT TYPE** | **3. DATES COVERED** *(From - To)* |
|---|---|---|
| 31 January 2012 | Final | 1 July 2003 – 1 July 2011 |

**4. TITLE AND SUBTITLE**

Benchtop Energetics: Research Progress, Concept Evaluation, and Apparatus Development

**5a. CONTRACT NUMBER**

**5b. GRANT NUMBER**

**5c. PROGRAM ELEMENT NUMBER**
61102F

**6. AUTHOR(S)**

Mario E. Fajardo, William K. Lewis III, Voncile L. Ashley, Rachel M. Nep, Emily C. Fossum, Christopher D. Molek

**5d. PROJECT NUMBER**
2303

**5e. TASK NUMBER**
EM

**5f. WORK UNIT NUMBER**
02

**7. PERFORMING ORGANIZATION NAME(S) AND ADDRESS(ES)**
Air Force Research Laboratory
Munitions Directorate
Ordnance Division
Energetic Materials Branch (AFRL/RWME)
Eglin AFB, FL 32542-5910

**8. PERFORMING ORGANIZATION REPORT NUMBER**

AFRL-RW-EG-TR-2012-009

**9. SPONSORING / MONITORING AGENCY NAME(S) AND ADDRESS(ES)**
Air Force Research Laboratory
Munitions Directorate
Ordnance Division
Energetic Materials Branch (AFRL/RWME)
Eglin AFB, FL 32542-5910
Technical Advisor: Dr. Jennifer L. Jordan

**10. SPONSOR/MONITOR'S ACRONYM(S)**

AFRL-RW-EG

**11. SPONSOR/MONITOR'S REPORT NUMBER(S)**
AFRL-RW-EG-TR-2012-009

**12. DISTRIBUTION / AVAILABILITY STATEMENT**

**Distribution A**: Approved for public release; distribution unlimited. Approval Confirmation 96 ABW/-2012-0027, dated 07 February 2012

**13. SUPPLEMENTARY NOTES** **SUBJECT TO EXPORT CONTROL LAWS**
**DISTRIBUTION STATEMENT INDICATING AUTHORIZED ACCESS IS ON THE COVER PAGE AND BLOCK 12 OF THIS FORM.**
**DATA RIGHTS RESTRICTIONS AND AVAILABILITY OF THIS REPORT ARE SHOWN ON THE NOTICE AND SIGNATURE PAGE.**

**14. ABSTRACT**

This report documents the research progress on the Benchtop Energetics project, the evolution of the underlying scientific concepts, and the accompanying changes to the experimental apparatus, during the period 2003-2011. The current goals of this project are: (1) to develop laboratory bench-scale initiation techniques and spectroscopic/mass-spectrometric diagnostics to characterize the initiation mechanisms and reaction kinetics of energetic materials, and (2) enable high-throughput bench-scale testing and evaluation of candidate advanced energetic materials, including those available only in sub-gram quantities.

**15. SUBJECT TERMS**
Detonation, deflagration, diagnostics, TOFMS, laser ablation, hyperthermal

| **16. SECURITY CLASSIFICATION OF:** | | | **17. LIMITATION OF ABSTRACT** | **18. NUMBER OF PAGES** | **19a. NAME OF RESPONSIBLE PERSON** |
|---|---|---|---|---|---|
| **a. REPORT** | **b. ABSTRACT** | **c. THIS PAGE** | | | Mario E. Fajardo |
| UNCLASSIFIED | UNCLASSIFIED | UNCLASSIFIED | SAR | 55 | **19b. TELEPHONE NUMBER** *(include area code)* 850-882-9067 |

**Standard Form 298 (Rev. 8-98)**
**Prescribed by ANSI Std. Z39.18**

This page intentionally left blank

## TABLE OF CONTENTS

## LIST OF FIGURES

## LIST OF FIGURES (continued)

## LIST OF ACRONYMS & ABBREVIATIONS

| | |
|---|---|
| Atomic Force Microscopy | AFM |
| Air Force Office of Scientific Research | AFOSR |
| Combined hydro and radiation Transport diffusion Hydrocode | CTH |
| Detonation Chemistry Apparatus | DCA |
| Intensified gated Charge-Coupled Device | IgCCD |
| Kinetic Energy | KE |
| Laser Induced Fluorescence | LIF |
| Los Alamos National Laboratory | LANL |
| Micro-Channel Plate | MCP |
| Neodymium Yttrium Aluminum Garnate | Nd:YAG |
| National Research Council | NRC |
| Optical Parametric Oscillator | OPO |
| PentaErithritol TetraNitrate | PETN |
| Physical Vapor Deposition | PVD |
| Residual Gas Analyzer | RGA |
| Sandia National Laboratory | SNL |
| Scanning Electron Microscopy | SEM |
| Stainless Steel | SS |
| Time-of-Flight Mass Spectrometry | TOFMS |
| Zel’dovich-von Neumann-Döring | ZND |

## 1. INTRODUCTION

This report documents the research progress on the Benchtop Energetics project, the evolution of the underlying scientific concepts, and the accompanying changes to the experimental apparatus, during 2003-2011. The original stated research objectives were:

- Develop laboratory bench-scale initiation techniques and spectroscopic diagnostics to characterize the initiation mechanisms and reaction kinetics of nanometric energetic materials.
- Enable high-throughput bench-scale testing and evaluation of candidate advanced nanometric energetic materials, including those available only in sub-gram quantities.

These objectives have broadened over time to include non-spectroscopic chemical species diagnostics (*e.g.* time-of-flight mass spectrometry [TOFMS]), testing of candidate insensitive energetic materials, and the generation of experimental data for validation of modeling and simulation efforts, specifically: testing the small-scale limits of the "Zel'dovich-von Neumann-Döring" (ZND) detonation model in conventional energetic materials.

This report begins with the narrative and statement of work from the Original Research Proposal, with minor edits to permit unlimited distribution. We include the original schedule, starting from an empty laboratory, unchanged for its amusement value. Actually, we eventually accomplished most of the first- and second-year tasks. However, the third-year tasks were largely postponed or abandoned, due to unanticipated technical difficulties and the change in emphasis away from spectroscopic diagnostics, once it became clear that the more general TOFMS approach could prove successful.

The main section constitutes a Progress Report which begins with the design and construction of our experimental apparatus. We document the changes to the apparatus that accompanied the changing scientific objectives mentioned above. We detail our efforts to produce multiple laser driven flyers from a single sample coupon in order to achieve our objective of high-throughput testing. We present our more-and-less successful approaches to producing large numbers of nominally identical small-scale energetic materials samples. We show our application of photographic and spectroscopic diagnostics, including the disappointingly limited information content of the observed emission spectra which prompted us to abandon this technique. Our most significant results have come from the TOFMS apparatus, which has undergone a major physical transformation; one prompted by our developing understanding of the issues associated with adapting this technique to our specific situation. We report preliminary results on samples containing nanoenergetic ingredients obtained with the 1$^{st}$ generation TOFMS apparatus, and point the Reader to three recent publications describing the development and demonstrated capabilities of the 2$^{nd}$ generation TOFMS system.

We finish with a summary of Lessons Learned and Future Directions, which are intended to provide a frank assessment of the original proposed work, addressing both the promising and disappointing paths followed, as well as highlighting opportunities for future research efforts.

## 2. ORIGINAL RESEARCH PROPOSAL

### 2.A. Summary of Proposed Research

The incorporation of nanometric (sub-micron size) metal fuel and oxidizer particles into energetic materials is a promising approach to increasing significantly the systems-level performance of munitions. We propose to exploit the phenomenon of laser driven shock initiation of energetic materials to enable bench-scale testing of initiation mechanisms and energy-release reaction kinetics of nanometric energetic materials *via* methods which utilize a minimum of energetic material and which routinely yield rapid repetitive energetic events. Such a capability would accelerate the rate of development of novel nanometric energetic materials, which is presently limited by testing protocols requiring the consumption of large quantities of often rare and expensive materials.

Direct laser initiation of energetic materials involves a complicated combination of shock, electronic, and thermal effects which are very difficult to relate to real-world chemical-explosive-driven initiation processes. We will use laser driven flyer plates to decouple the laser photon flux from the energetic material, reducing interference from direct electronic and thermal initiation mechanisms, thus greatly simplifying matters. The technology for producing laser driven flyers is advancing rapidly, thanks to efforts in a number of laboratories around the world. We will exploit as much of the state-of-the-art as feasible, including the use of advanced numerical simulation techniques to model our benchtop experiments.

We will adopt the "nanoshock target array" approach for generating repetitive energetic events pioneered by Dlott and coworkers. In this method thin films of energetic materials are prepared on a transparent substrate "target coupon" which is rastered mechanically through the fixed focus of a pulsed laser beam. Our novel adaptation will include the laser driven flyer plate intermediate, and a target-in-vacuum capability. The expansion of reaction intermediates into vacuum will quench subsequent reactions and preserve these intermediates for spectroscopic interrogation. Conversely, we will also employ buffer gases and "glass confined" experimental geometries as necessary to permit longer reaction times. The spectroscopic diagnostics will permit testing of common modeling assumptions, such as local thermodynamic equilibrium, and will be capable of measuring conditions in the reacting flow such as rotational and vibrational temperatures. By making these direct measurements on reacting nanometric energetic materials, we hope to develop an improved understanding of their energy-release reaction kinetics, and so answer important qualitative questions such as: "do nanometric metal fuel particles actually react faster than micron-scale particles, and does this really matter?"

### 2.B. Proposal Introduction

The incorporation of nanometric (sub-micron size) metal fuel and oxidizer particles into energetic materials is a promising approach to increasing significantly the systems-level performance of munitions; *e.g:*. replacing inert metal munition components with energetic Reactive Fragments, Blast-Enhancing Liners, and Structural Reactive Cases [1-2]. These advances in combination promise to <u>double</u> the total chemical energy content of a munition, and to increase by nearly an <u>order of magnitude</u> the destructive energy coupled to some targets.

A serious impediment to the timely development of novel nanometric energetic materials is the present requirement of producing and accumulating large quantities of typically rare and expensive material for testing purposes; *e.g.*: each Reactive Fragment test item weighs tens of grams, and each Structural Reactive Case test item weighs several kilograms. Also, due to safety and logistical considerations, current explosives-driven testing methods are limited to at best a few energetic events per day. Thus, our primary objective is to "**develop laboratory bench-scale initiation techniques and spectroscopic diagnostics to characterize the initiation mechanisms and reaction kinetics of nanometric energetic materials**" *via* methods which utilize a minimum of material and which routinely yield rapid repetitive energetic events. When brought to maturity, such a capability should greatly accelerate the evaluation process for candidate nanometric energetic materials, and should contribute to a more complete fundamental understanding of their energy release mechanisms.

### 2.C. Laser Driven Flyers & Shocks

Our proposed approach is to use the high peak powers available from pulsed lasers to drive miniature flyer plates which subsequently produce shocks capable of initiating chemical reactions in energetic materials [3-6]. Direct laser initiation of energetic materials involves a complicated combination of shock, electronic, and thermal effects which are very difficult to relate to real-world chemical-explosive-driven initiation processes [7]. The miniature flyer plate intermediate decouples the laser photon flux from the energetic material, reducing interference from direct electronic and thermal initiation mechanisms, thus greatly simplifying the initiation conditions.

Laser driven flyer plate technology has experienced considerable advancement over the past decade [8-24]. The simplest experimental configuration is shown in Figure 1a; with all experiments conducted in vacuum unless stated otherwise. In our proposed nominal implementation a 2 Joule, 1064 nm, 10 ns duration pulse from a Q-switched Nd:YAG laser is focused through a millimeters-thick transparent substrate to a 2 mm diameter circular spot at the interface between the substrate and a 10 micron thick metal film. The corresponding incident laser fluence is $\approx 60$ J/cm$^2$, and the average incident laser intensity is $\approx 6 \times 10^9$ W/cm$^2$, which is close to the limit imposed by dielectric breakdown in likely (BK7 glass, fused silica, *etc.*)

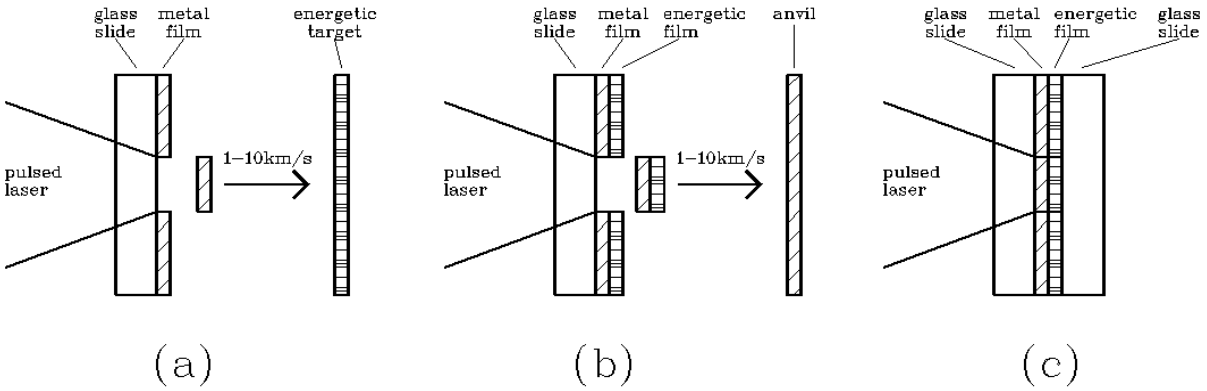


**Figure 1. Experimental configurations (not to scale)**

substrate materials [12]. The leading edge of the laser pulse is absorbed in a thin (~ 1 micron [17]) layer of the metal film, vaporizing this layer and producing a high-temperature high-pressure plasma which efficiently absorbs the remainder of the laser pulse [11], further heating the plasma. The plasma drives two shock waves, one into the thick substrate and one into the thin metal film, opening the interface [11,12]. When the yield strength of the unvaporized portion of the metal film is exceeded, a circular flyer is sheared out of the metal film and further accelerated by the expanding plasma over a ~ 100 ns period to a final velocity of several km/s [10-13,15,16]. We can use a simple one-dimensional model [11] to estimate the plasma pressure at the end of the nominal laser pulse as ≈ 40 kbar, and the final flyer velocity as ≈ 3 km/s, for our nominal aluminum flyer. The kinetic energy of this nominal 80 μg aluminum flyer is ≈ 0.4 J, which is 20 percent of the incident laser energy. Beyond this nominal single-layer flyer, we will also attempt to exploit advances in the production of multilayer flyers, which offer advantages such as: improved laser energy absorption, thermal and electronic insulation of the metal flyer from the driving plasma, and shock wave buffering [10,14-16,18,22-24].

It is well known that a "flat top" or "top hat" focused laser beam transverse intensity profile, *i.e.* constant central intensity with sharply defined edges, is highly desirable for accelerating these metal flyers. Flyers produced using a flat top profile beam focus can travel intact for several millimeters in vacuum [13]. In contrast, flyers produced by single-lens focusing of Gaussian profile laser beams show significant non-planarity and loss of structural integrity after traveling only a few hundred microns [19]. Fortunately, pulsed Nd:YAG lasers are commercially available (*e.g.* for pumping other solid state lasers or optical parametric oscillators) with approximately flat-top beam profiles in the near field, which can be transformed to flat-top focused beam profiles by the relay imaging technique [25]. We will attempt fine tuning of the focused beam intensity profile by a variety of "beam shaping" optical techniques [26-37]; at present, lossless refractive methods employing aspheric lenses seem the most applicable to the high intensity laser pulses in question [32-37].

Laser driven flyers produced under similar conditions have been used to produce shocks capable of initiating primary and secondary high explosives [7,10,20,21]. We estimate the shock conditions induced in an energetic target by the impact of our nominal aluminum flyer plate via the "impedance matching" method [38-41]. Taking the flyer to be made of 6061-T6 Al alloy and traveling at 3 km/s, and the stationary target to be dilute nano-Al/Teflon, we calculate a peak shock pressure in the Teflon of ≈ 200 kbar, albeit with a supported duration of under 4 ns (*i.e.* 2*flyer thickness/shock velocity in Al). We will perform experiments in the geometry of Figure 1a to determine if these conditions can initiate exothermic chemical reactions in the energetic materials of interest.

Another promising experimental configuration is depicted in Figure 1b, in which a thin film of energetic material (*e.g.* nano-Al/Teflon, epoxy-bound nanometric metal/metal oxide mixtures, nanolaminate mixed metal systems, *etc.*) is coated directly onto the flyer plate material; this geometry mimics the explosive-driven launch of a Reactive Fragment. In this case the energetic material is accelerated on the much longer ~ 100 ns plasma expansion timescale discussed above, and is subjected to much weaker shock pressures. However, in this experiment the energetic material is subjected to multiple shock reverberations [14,22,24], as well as to strong shearing forces as it is punched out by the metal flyer. {The reflection of a compression

wave at a boundary with a lower shock impedance material (*e.g.* Al:Teflon and Telfon:vacuum) results in a backwards traveling release or "rarefaction" wave, and hence to tensile stresses which can lead to coating debonding [42] and perhaps to spalling or "scabbing" of the coated flyers [43,44].} Again, we are unsure whether these launch conditions will initiate exothermic chemical reactions in the energetic coatings. However, we note that simply by varying the thickness of the underlying metal film we can bridge from the flyer plate regime (several microns-thick films) to the laser-driven exploding foil regime (sub-micron films) to the direct laser initiation regime (no film). Thus, we are confident that we can find effective initiation-upon-launch conditions, as necessary. Coated flyers which survive the launch process intact will impact a variable thickness metal anvil, again mimicking the high-shock high-shear target interactions of a Reactive Fragment.

In order to better quantify the shock/shear/thermal loading history of the energetic material, we will pursue theoretical numerical simulations of the laser driven flyer launch and target interaction processes. We will use the CTH hydrocode (which actually includes models for materials strength and fracture [45]) to simulate our experiments. We will compare as many experimental observables as possible (*e.g.* flyer geometry and velocity, recovered coupons and targets, spectroscopically measured pressures and temperatures, *etc.*) with the predictions of the simulations seeking, at a minimum, internal self consistency. These simulations should also identify flyer/target configurations prone to problems such as spalling of the energetic coating upon shock reflection from the free surface, and will guide the use of multilayer flyer structures to mitigate these problems.

An important attraction of the launch-initiated coated flyer configuration depicted in Figure 1b is the possibility of preserving early reaction intermediates and products for spectroscopic study by quenching of the reacting flow during the expansion into vacuum [46]. However, this expansion quenching process also obviously interferes with the exothermic chemical reactions of interest, cutting off the reaction progress on nano- to micro-second timescales. This problem has lead others to study direct laser-initiated energetic reactions in high pressure confined geometries [47-50]; although quenching by thermal conduction to the confining materials also affects the reaction kinetics on micro- to milli-second timescales [51-53]. Thus, we also propose to perform <u>laser driven shock</u> experiments with the metal "flyer" layer and energetic material coating in a "glass confined" arrangement, as depicted in Figure 1c, in order to extend the reaction times as desired. We will seek to answer important qualitative questions such as: "do nanometric metal fuel particles actually react faster than micron-scale particles, and does this really matter?" If the rate limiting step for energy release is to be found among the subsequent longer timescale reactions, any early reaction accelerations obtained by incorporating nanometric ingredients may be mooted.

Our solution to the problem of producing repetitive energetic events is taken directly from conversations with AFOSR contractor Prof. Dana Dlott of the U. of Illinois at Urbana-Champaign, who has employed "shock target arrays" for over a decade in condensed phase ultrafast laser spectroscopic experiments [54-63]. As shown in Figure 2, by rastering the position of a large coated substrate transverse to the fixed laser beam, hundreds of successive energetic events can be generated at the repetition rate of the laser [64]. An obvious advantage of this approach is that it consumes only small quantities of energetic materials; perhaps

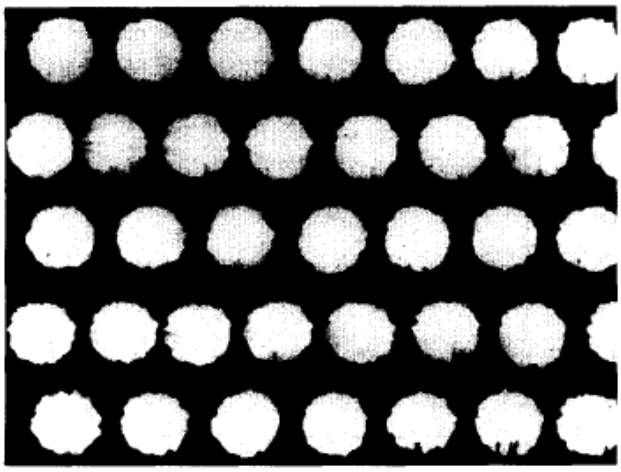

**Figure 2. Substrate after 36 laser irradiations**
*The spots are 2 mm in diameter [64].*

~ 100 mg to produce a 5 cm x 10 cm x 10 micron film coating, with each such coated substrate coupon yielding about 1000 flyers, each flyer carrying ~ 100 μg of energetic material. At a nominal maximum laser repetition rate of 10 Hz, each coupon could be consumed in as little as 100 seconds; then a replacement coupon could be inserted and data acquisition resumed in a matter of minutes. This ready availability of rapid, repetitive signals should greatly facilitate the development of our experimental diagnostics, and ultimately allow for a high throughput of samples for evaluation. In fact, a secondary technical objective of this program is to "**enable high-throughput bench-scale testing and evaluation of candidate advanced nanometric energetic materials, including those available only in sub-gram quantities."** We will not attempt to duplicate Prof. Dlott's, or others' [65-67], ongoing condensed phase ultrafast laser spectroscopic studies; rather we will add the novel element of utilizing shock target arrays in vacuum, combined with nanosecond resolution spectroscopic diagnostics to follow the subsequent exothermic chemical reaction kinetics.

### 2.D. Microscopic, Photographic, and Spectroscopic Diagnostics

Our initial experimental diagnostics will rely upon available laboratory equipment and existing in-house analytical capabilities. We hope to demonstrate the utility of our methods in the early stages of this program, to justify the proposed acquisition of more sophisticated experimental diagnostics.

We have previously employed scanning electron microscopy (SEM) of laser ablated thick metal targets to characterize the shapes of the "craters" produced at the metal/vacuum interface by the ablation process [68]. During the initial alignment of our laser driven flyer apparatus we will make similar measurements on opaque thick metal targets, using the SEM and atomic force microscopy (AFM) instruments available in-house at AFRL/MNME. We hope to distinguish between crater geometries produced using a laser focus with a good top-hat intensity profile (*e.g.* relay imaging) *vs*. deliberately poorly focused cases (*e.g.* single lens focusing). We will also make microscopic examinations of the holes left behind in the metal films after laser driven flyer

launch from coated transparent substrates [13,64], for comparison with the final structures calculated in the numerical simulations.

The velocities and structural integrity of plain metal flyers will be determined from high speed optical images produced using a newly acquired intensified gated charge-coupled device (IgCCD) camera with a minimum exposure time of 5 ns. Side-view images will be recorded at various delays following the Nd:YAG driving laser pulse, and velocities calculated as the distance traveled divided by the delay. Similar images will be recorded for coated flyers, and for bare flyers impacting energetic targets. These measured velocities will provide the first checks of the theoretical numerical simulations. End-on images of the target will be scrutinized for the circularly symmetrical appearance of the breakthrough of the laser plasma around the flyer perimeter; the appearance of plasma emissions elsewhere signals the disintegration of the flyer [19]. The time-dependent reflectivity of the metal flyers will also be measured using a continuous wave HeNe laser and a fast photodiode, as an alternative measure of flyer planarity and structural integrity.

We will monitor the progress of the energy release reaction kinetics via high speed photographic and spectroscopic measurements of the appearance of reaction intermediates and products. These studies can be considered as long-time (nano- to milli-second) extensions of the ultrafast laser studies on "nanoshocked" energetic materials pioneered by Dlott and coworkers [54-63], with our original contribution being the marriage of laser driven shock initiation with gas-phase spectroscopic techniques. For example, in the experiments depicted in Figure 1b, we will use the IgCCD camera to produce images of the coated flyers in flight through vacuum and after impact on a target. If the energetic material can be made to initiate upon launch, then luminescence from the reacting material (note that the flyer metal must be different from that in the energetic coating to reduce spectral interference from the laser driven plasma) will reveal whether high peak shock pressures (at the center of the flyer) or high shear rates (at the edge of the flyer) are responsible; this qualitative result would be of immediate value to Reactive Fragment munitions designers for whom initiation upon launch is an undesirable occurrence.

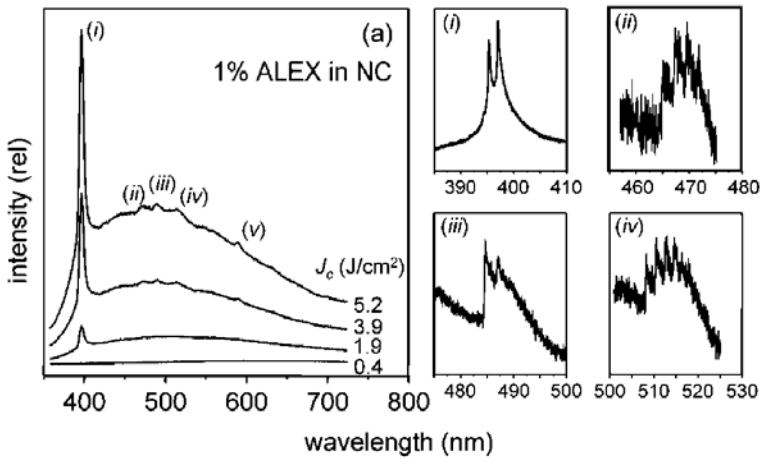


**Figure 3. Time integrated emission spectra from laser-ignited nano-Al/nitrocellulose** *(i) is an Al atom emission, (ii)-(iv) are vibronic transition of hot AlO, (v) is a Na impurity [63].*

Once the spatial locations of the sources of luminescence are known, we will attach the IgCCD to a spectrometer and record time-resolved and position-dependent wavelength-dispersed emission spectra of any luminescent species present in the reacting flow. As shown by the time- and position-integrated emission spectra in Figure 3, spectral analysis should at the very least reveal the identities of some of the electronically excited reaction intermediates and products. Our use of shock initiation and vacuum expansion combined with time- and position-resolved emission detection should allow us to reduce spectral interference from the broad continuum emission which dominates the spectra shown in Figure 3; in laser ablation experiments such emissions originate from hot dense plasma regions very near to the ablated surface, and decay much more rapidly than the atomic and molecular emissions of interest [68]. With these spectroscopic diagnostics in place, we will perform experiments launching coated flyers into vacuum, into inert atmospheres, and into air to test the hypothesis that "afterburning" with ambient oxygen [69] contributes to the anomalously high total energy release observed for certain Reactive Fragment candidate formulations.

The availability of a second tunable nanosecond laser system will enable considerably more powerful spectroscopic diagnostics for characterizing both the shock initiation conditions and the gas phase reaction kinetics. While (sub)picosecond resolution is required for properly characterizing the time dependence of condensed phase shock-induced processes on the molecular length scale [54-63,65-67], nanosecond lasers have recently been used to measure shock pressures in laser-driven 80-μm-thick Teflon films via spontaneous Raman spectroscopy [70-72]. We are also anxious to apply gas-phase laser induced fluorescence and transient absorption diagnostics that can probe for non-emitting molecular species, which could represent the majority of the material in the reacting flow [73]. These spectroscopic measurements would provide independent tests of modeling assumptions such as local thermodynamic equilibrium, and could yield detailed information, *e.g.*: rotational and vibrational temperatures of the various reaction intermediates and products [74]. Parametric experiments would also yield directly the dependence of the energy releasing reaction kinetics on the particle sizes of the nanometric energetic ingredients. Throughout this effort we will continue to evaluate opportunities to apply new spectroscopic diagnostics.

### 2.E. Proposed Statement of Work

This work will be performed in-house at the AFRL/MNME Energetic Materials Branch; laboratory space with the required utilities is currently being upgraded in Bldg. 1200, Rm. 11.

FY03 Preaward Activities:

We have already initiated the procurement of a 2 Joule Nd:YAG laser pumped optical parametric oscillator (OPO) system. The Nd:YAG laser will be used in our initial laser driven flyer experiments, in order to determine the suitability of this class of laser for this role. The future acquisition (FY05) of a dedicated flyer launch laser will be illuminated by this experience, with the first Nd:YAG laser ultimately returning to its designed role of pumping the tunable OPO system. We have also secured funding for the acquisition of a 0.3 meter focal length spectrometer equipped with an intensified gated CCD (IgCCD) array detector. This IgCCD detector will also serve as a fast optical camera with a 5 ns shutter speed. Preliminary experiments will be performed in a salvaged vacuum chamber using existing vacuum pumps.

FY04 Objectives:

The main objectives in FY04 are to complete the design, procurement, setup, and testing of an interim experimental apparatus, and to begin launching flyer plates and characterizing them with available preliminary diagnostics. We will also complete the design and procurement of the components of the final experimental apparatus (excepting the 2nd generation flyer driving laser). Specific experimental milestones include: (1) production of metal film coated transparent substrates, (2) launching of laser-driven flyer plates with the 2 J Nd:YAG laser, and (3) recording of images of the flyer plates with the IgCCD camera.

We will begin with vapor deposition of metal films onto glass microscope slides, and progress to thermal in-vacuum diffusion bonding of metal foils [13,23]. We will evaluate any damage to these coated substrates during flyer launch, and find substrates and launch conditions conducive to the production of multiple flyers in succession from adjacent spots on a single target coupon. We will record images of the flyer plates in vacuum with the IgCCD camera, and determine achievable velocities *vs*. metal film thickness and laser parameters. We will examine the structural integrity and planarity of the flyers. We will investigate requirements for any additional laser beam shaping beyond that provided by the relay imaging method. We will attempt to initiate reactions in energetic materials via flyer impact in vacuum.

FY04 Tasks:

1. Procure and set up optical tables.
2. Set up and test 2 J Nd:YAG laser and optical parametric oscillator system.
3. Set up and test IgCCD camera & spectrometer system.
4. Design, procure, and set up vacuum metal film deposition system; deposit films onto transparent substrates.
5. Set up and test (salvaged) interim experimental vacuum chamber.
6. Design, procure, set up, and test laser relay imaging optical system.
7. Launch and photograph bare metal flyers.
8. Attempt initiation of energetic materials via flyer impact; record images and emission spectra.
9. Design and procure permanent main experimental vacuum chamber.
10. Design and procure in-vacuum sample scanning system.
11. Procure spin coater and drying oven.

FY05 Objectives:

In FY05 we will complete the assembly and testing of the permanent version of the main experimental apparatus, and will proceed to the production, launching, and spectroscopic characterization of coated flyers. We will begin the expansion of our Benchtop Energetics Team to include computational support, and hands-on participation by a Lab Technician. We will also use the lessons learned in FY04 to formulate the requirements for (beam quality, pulse energy, pulse duration, repetition rate, *etc.*), and initiate procurement of, the 2nd generation flyer driving laser. Specific experimental milestones include: (1) production of target coupons coated with energetic materials, (2) rapid repetitive launching of coated flyer plates, and (3) recording of images and emission spectra of coated flyer plates.

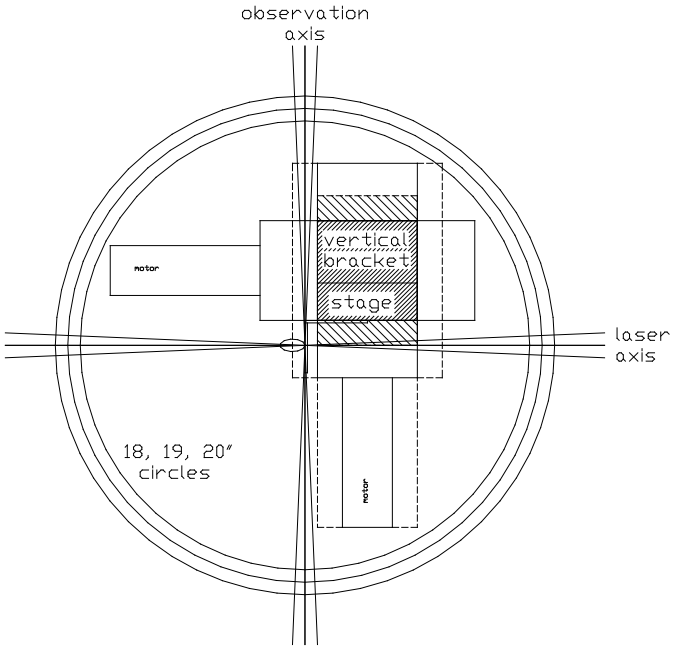


**Figure 4. In-vacuum XYZ translation system**
*Laser shown incident from the right.*

We will produce nanometric energetic film coatings on metal coated substrates *via* spin coating and spray coating methods. Teflon AF is an amorphous fluoropolymer which is soluble in certain fluorinated solvents and can be spin cast into pinhole-free thin films [75]. We will produce Teflon coatings containing nanometric and micron-scale metal fuel particles. We will attempt spin coating of epoxy-bound metal/metal oxide systems, experimenting with various solvents to thin the epoxy. We will also attempt direct vapor deposition of mixed metal nanolaminates in-house. We will pursue collaborations with any AFOSR sponsored contractors interested in sending us their materials for testing.

Figure 4 shows our straw-man design of an in-vacuum XYZ motorized positioning system, which also gives an indication of the size of the final experimental vacuum chamber. The two horizontal stages will accommodate up to 5 cm of motion, while the vertical stage will move up to 10 cm. The stage moving parallel to the laser beam axis permits fine adjustment of the laser spot focusing conditions, as the relay imaging optics are required to remain fixed. Within this apparatus, we will launch coated flyer plates with the 1st generation 2 J Nd:YAG laser, and record images with the IgCCD camera located along the observation axis (side view) and slightly off the laser axis (end view). We will determine achievable velocity *vs*. energetic coating thickness and laser parameters. We will determine the structural integrity of the coated flyers; looking for planarity, spalling, *etc*. We will determine if the launch conditions are sufficient to initiate the energetic coating materials, or if impact of the coated flyers onto a target is required. We will record emission spectra of any luminescence from the initiated energetic materials, and explore the role of metal particle size on the reaction kinetics. We will determine the technical requirements for the 2nd generation flyer launch laser.

FY05 Tasks:

1. Perform theoretical simulations of laser driven flyer launch process.
2. Setup and test permanent main experimental vacuum chamber.
3. Setup and test in-vacuum sample scanning system.
4. Produce target coupons coated with energetic materials.
5. Launch and photograph coated metal flyers in vacuum.
6. Determine initiation conditions for coated flyers.
7. Record emission spectra of coated flyers.
8. Launch and characterize coated metal flyers in inert and oxidizing atmospheres.
9. Begin development of multilayer flyers.
10. Procure 2nd generation flyer launch laser.

FY06 Objectives:

By FY06 the lab facilities buildup phase will be largely completed, and our main objectives will be to expand the Benchtop Energetics group *via* the addition of an NRC Postdoc, and to accelerate the pace of experimentation. Specific experimental milestones include: (1) spectroscopic characterization of condensed phase initiation conditions, and (2) recording of laser induced fluorescence (LIF) and transient absorption spectra of laser-initiated nanometric energetic materials.

These two-laser techniques will permit the characterization of non-luminescing species, such as ground state atoms and molecules. Measurements of rotational and vibrational temperatures of the various species will be compared with the predictions of the theoretical models. The dependence of the energy releasing reaction kinetics on the particle sizes will be determined.

FY06 Tasks:

1. Continue theoretical simulations of laser driven flyer launch process.
2. Continue development of multilayer flyers.
3. Setup and test 2nd generation flyer launch laser.
4. Spectroscopic characterization of shock conditions upon launch of coated flyers.
5. Record LIF and transient absorption spectra of laser-initiated nanometric energetic materials.
6. Determine effect of constituent particle size on reaction kinetics.

## 3. RESEARCH PROGRESS

Most of the results included in this report have appeared in a number of oral and poster presentations [76-88], culminating in a recent series of archival written publications [89-91]. We present this material organized, with the benefit of hindsight, into a form which we hope conveniently summarizes both our successes and failures. The intent is to provide a valid starting place for future efforts in this field, addressing both the promising and disappointing paths followed. We include original notebook references, *e.g. [AB1234]*, where available.

### 3.A. Apparatus Construction

#### 3.A.1 Main Vacuum Chamber

As discussed above in the Proposal, our experimental approach can be seen as a milligram and microsecond extension of prior thin-film ultrafast-laser-driven energetic materials experiments [54-67] -- enabled by a sample-in-vacuum configuration. We seek to characterize the molecular debris emerging from these small-scale energetic events for further clues on the progress of the chemical reaction kinetics. The rapid expansion into vacuum cools and then disperses the intermediates and products. This quenches the chemistry, thus preserving the gaseous species for interrogation. We expect to acquire qualitatively different and complementary information to that obtained from the ultrafast measurements, as well as from more traditional small-scale initiation studies.

Implementing a sample-in-vacuum capability required the design and construction of a high-vacuum chamber and pumping system, as shown in Figure 5. The scale of the vacuum chamber is set by the size of the XYZ sample translation system shown above in Figure 4. The four 6-inch and four 2.75-inch Conflat ports centered 12 inches above the optical table provide optical access for the driver laser beam and for the photographic and spectroscopic diagnostics. The other four 6-inch Conflat ports are used for pumping, and for electrical feedthroughs to the XYZ translator. A single 500 l/s turbopump, backed by an oil-sealed rotary vane mechanical pump, yields a base pressure in the mid-$10^{-6}$ torr range. A residual gas analyzer (RGA) helps to find and fix air leaks, and registers water vapor as the main background gas species.

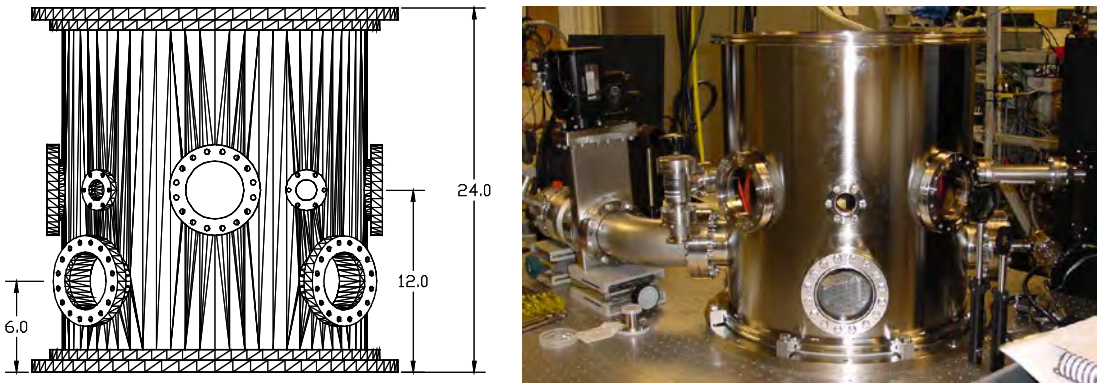


**Figure 5. Main experimental vacuum chamber**
*Dimensions given in inches. [WL1044]*

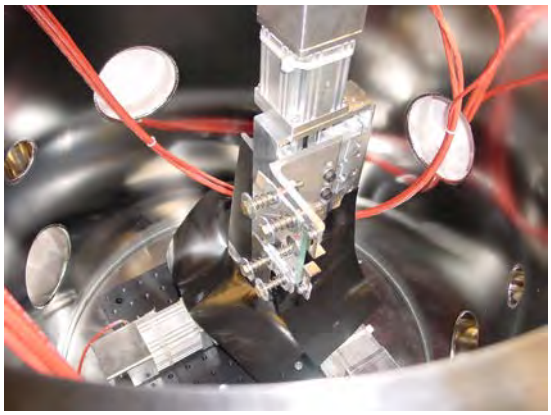

**Figure 6. In-vacuum XYZ translator**
*Shown with glass target in 1st generation sample coupon holder. [WL1046]*

Figure 6 shows a close-up of the in-vacuum XYZ translator, as well as the 1st generation homemade spring-loaded sample coupon holder. The sample coupons are assembled from commercially available nominally 2x3x¼ inch (51x76x6 mm) glass optical windows, onto which thin (10-100 μm) metal foils are either bonded by an adhesive, or grown directly by physical vapor deposition. The XYZ translator permits raster scanning of the assembled coupons through the fixed focus of the flyer driving laser beam, with a stated positioning accuracy of ± 1 μm.

### 3.A.2 Laser Optics

Figure 7 shows the optical table layout, including the pulsed Nd:YAG laser system (lower left) with a custom side exit port for the 1064 nm fundamental. This beam transits a Faraday isolator (lower right) and then is sent to the main chamber in the background *via* high-intensity mirrors arranged into two periscopes to match the 12-inch height of the vacuum ports.

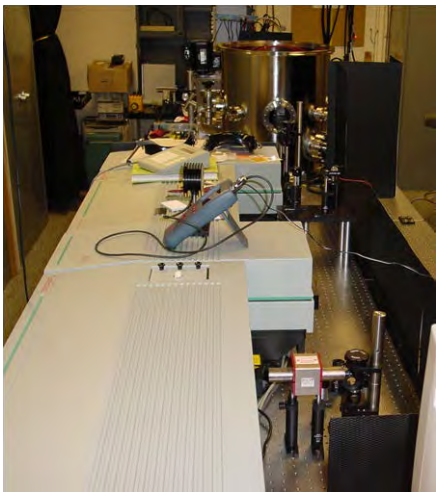

**Figure 7. First optical table setup**
*View shows laser system, optics, and main chamber. [WL1044]*

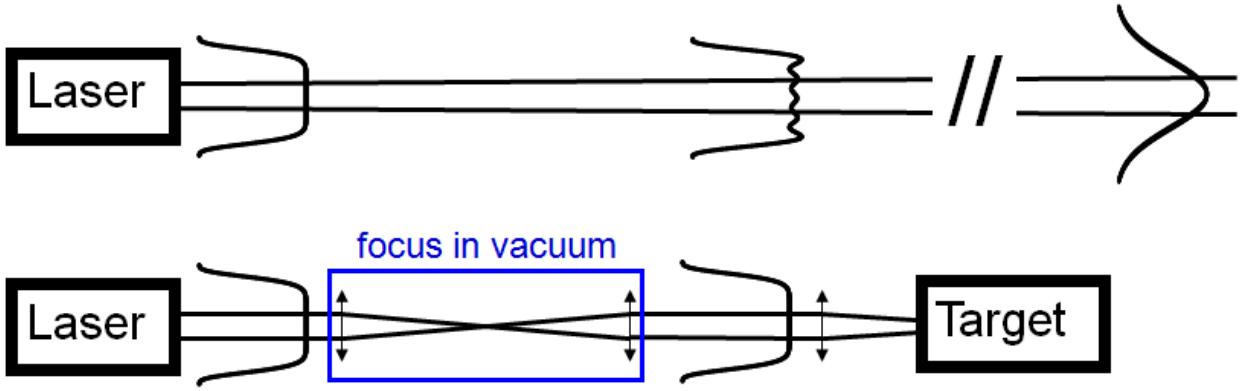


**Figure 8. Relay imaging cartoon**

As discussed in the Proposal, a "flat-top" or "top-hat" laser beam transverse intensity profile is desirable for launching the laser driven flyers [13,19]. Our Nd:YAG laser was originally designed for pumping an optical parametric oscillator (OPO), and produces a 9-mm-diameter output beam with an approximately "top-hat" near-field intensity profile. The top panel of Figure 8 depicts the evolution of the propagating beam profile due to diffraction effects [92]. The mid-field intensity profile, with concentric bright and dark rings is evident after ~ 1 m beam travel; our earliest experiments were performed by focusing such beams with the target in the convergent portion of the beam. We quickly implemented a relay imaging scheme (lower panel of figure 8) to reconstruct a top-hat intensity profile just outside the main vacuum chamber.

Figure 9 shows the optical table layout for relay imaging the output face of the last Nd:YAG amplifier rod to the focusing lens located 2.8 m downstream, just outside the main chamber. Actually, the optical path is shown reconfigured to employ the 2nd Nd:YAG laser which was incorporated in 2007. We use two 1064 nm anti-reflection coated lenses with effective focal lengths of 0.69 m at the 1064 nm laser wavelength. The long cross-shaped secondary vacuum chamber is required to avoid dielectric breakdown of air at the laser focus.

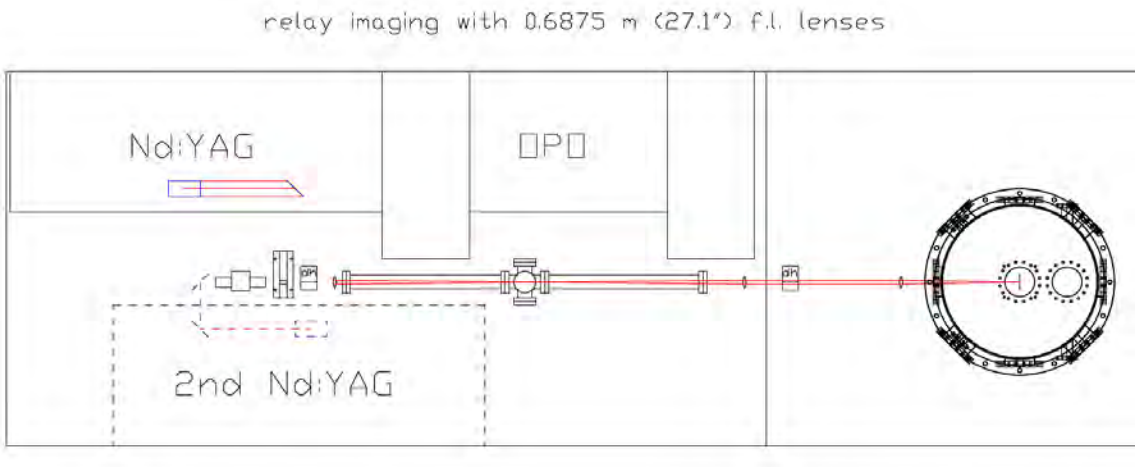


**Figure 9. Relay imaging schematic c2007** *[WL1061]*

**Figure 10. Laser beam profiles from beam camera and burn paper**
*Left and center -- beam at chamber without relay imaging, right -- relay imaged. [WL1056 & WL1061]*

Figure 10 shows the laser beam profiles at the final focusing lens just outside the main chamber entrance, with and without the relay imaging optics. The image in the left panel is from a laser beam camera, the center and right images are marks made in laser burn paper. Both the left and center images show the expected concentric diffraction rings, which are much subdued in the right side image. In our experiments performed prior to June 2010 we used a variety of lenses to focus this beam onto the target, which again remained in the convergent part of the beam, resulting in non-flat-top focused intensity profiles at the target.

In June 2010 we were informed of a simpler and more effective approach to obtaining a focused flat-top beam intensity profile at the sample target [93]. As shown in figure 11, we have removed the relay imaging optics, and currently use a single 40 cm focal length lens, placed ≈ 48 cm from the target surface, to image the output face of the Nd:YAG laser final amplifier rod directly onto the target at ≈ 0.15x magnification. In this case, the tightest laser focus occurs in the main vacuum chamber ≈ 8 cm above the ≈ 1.4-mm-diameter imaged spot at the target surface. This configuration is used in all the experiments reported in refs. [86-91].

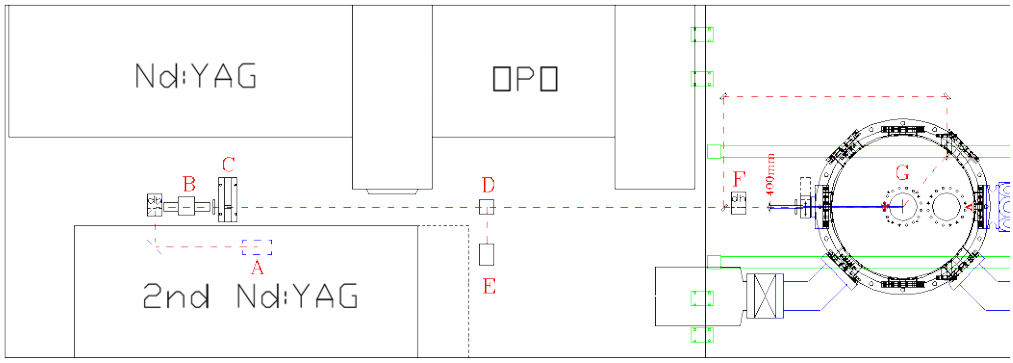


**Figure 11. Single-lens imaging schematic c2010**
*A - Nd:YAG amplifier rod, B - Faraday Isolator, C - pulse-picking flip mirror, D - continuously variable attenuator, E - beam dump, F - periscope, G - sample target. [EF02065, MF12059]*

### 3.B. Laser Driven Flyers

Figure 12 shows an early attempt at launching and photographing laser driven projectiles in air. The badly distorted "flyers" are punched out of the ≈ 70-μm-thick protective polyethylene film covering the nominally 250-nm-thick reflective Al coating on the 51x76x6 mm Al/soda-lime-glass mirrors. The laser pulse energy of $E_{laser} \approx 1.2$ J/pulse, delivered through the glass over a pulse duration of $\tau \approx 10$ ns and focused to a d ≈ 3-mm-diameter spot, yields an incident intensity at the Al:glass interface of $I_{laser} \approx E_{laser} / (¼ \pi d^2 \tau) \approx 7x10^9$ W/cm$^2$. Rather surprisingly, as shown in Figure 13, the soda-lime glass substrates transmit this enormous laser intensity without incurring visible damage from dielectric breakdown, making them the foundation for relatively inexpensive and rugged target coupons. These experiments also gave us hope of achieving our objective of producing nominally "identical," repetitive events, yielding fairly reproducible polymer "flyer" velocities of $v_{flyer} = 930(50)$ m/s (standard deviation in parenthesis).

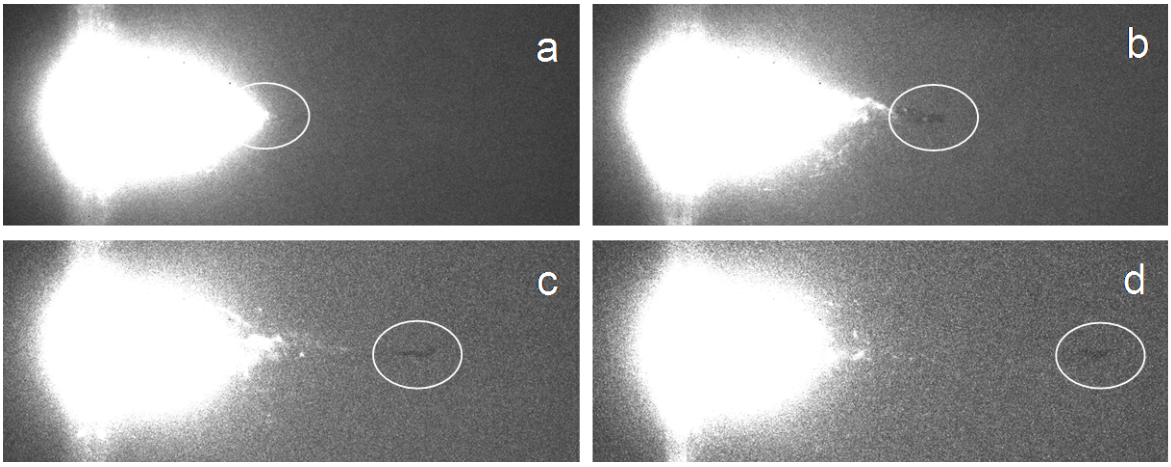


**Figure 12. Polyethylene "flyers" in air**
*The field of view for each image is ≈30 mm wide; shown with laser incident from left. IgCCD exposure duration = 100 ns, delays: (a) 10, (b) 15, (c) 20, (d) 25 μs. [WL1032]*

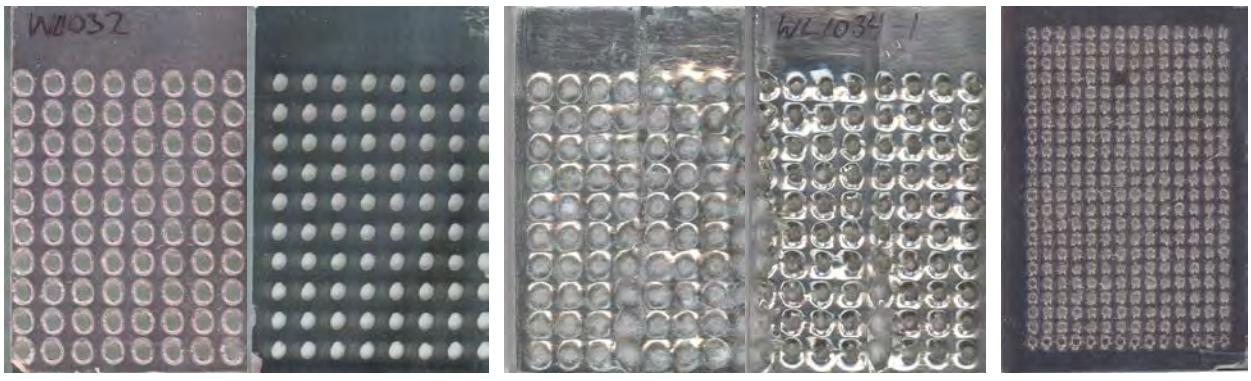


**Figure 13. Recovered sample targets**
*Left and right -- soda-lime glass mirror covered with 70-μm-thick protective polyethylene film. Center -- float plate glass covered with 75-μm-thick dead-soft aluminum tape. Each coupon measures 76x51 mm. [WL1032, WL1034, WL1053]*

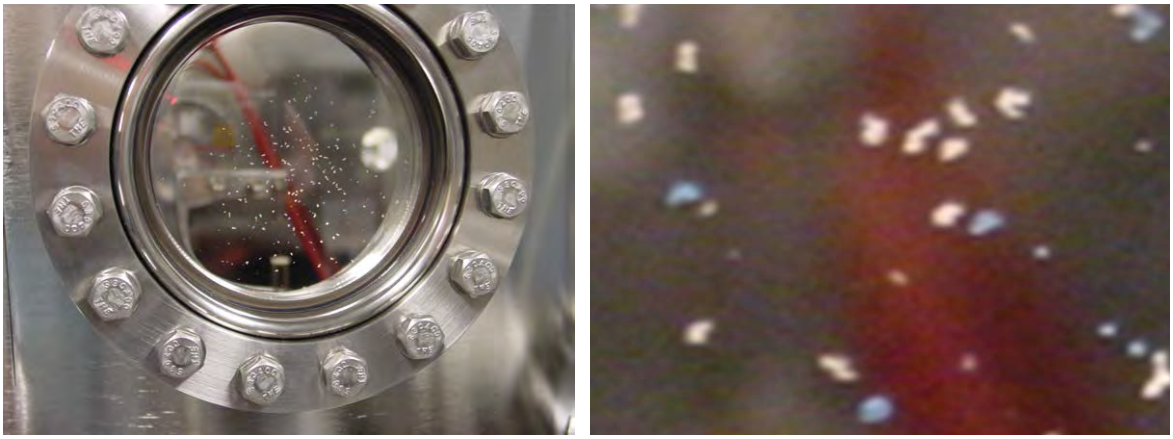

**Figure 14. Polyethylene "flyers" stuck to vacuum chamber window** *[WL1053]*

Figure 14 shows several of the polyethylene "flyers," launched from the target shown in the right panel of Figure 13, stuck to the vacuum chamber window after transiting ≈ 30 cm in air. Initially, these experiments supported the viability of our envisioned approach to "… employ buffer gases … to permit longer reaction times" mentioned above in Section 2.A. However, we found that the main chamber eventually became filled with a thin smoke upon continued firing of the flyer driving laser. With this smoke present, we observed erratic flyer velocities, which coincided with our visual observation of dielectric breakdown in the smoky air above the substrate target (in the convergent portion of the laser beam). Thus, it seemed to us that, for occupational safety reasons alone, working in a buffer gas environment would require a purpose-built system for circulating and filtering the gas in the main chamber. Instead, we abandoned this approach, and proceeded with our plans to work with samples-in-vacuum, exclusively.

Figure 15 shows the damage to the glass viewport opposite the laser entrance port caused by impact of titanium fragments (launched from 13-μm-thick Ti foil) after transiting ≈ 30 cm in vacuum. Fortunately, the distinctive noise made by the first impact event ("tink!?!") was sufficient to alert us to terminate this experiment prior to catastrophic failure of the window.

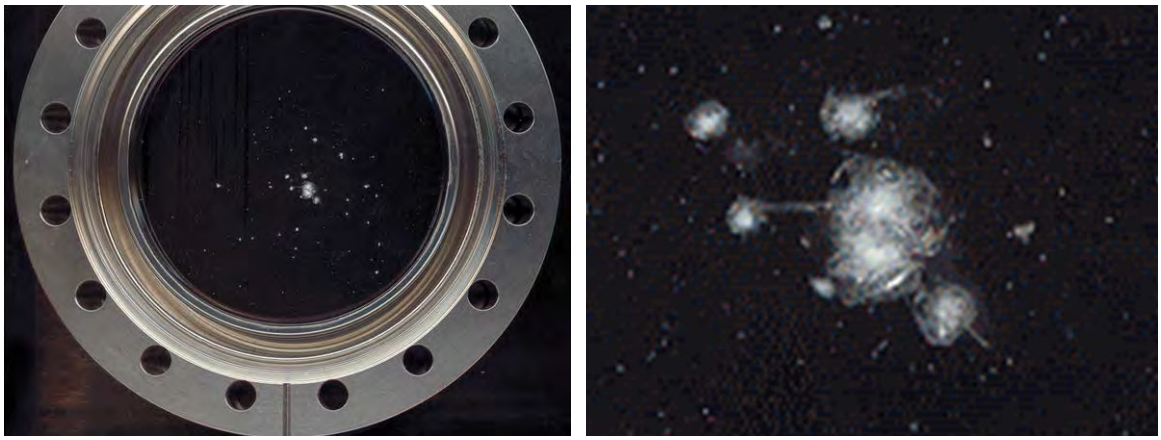

**Figure 15. Damaged glass viewport**
*Pitting caused by impact of Ti flyer fragments. [WL1064]*

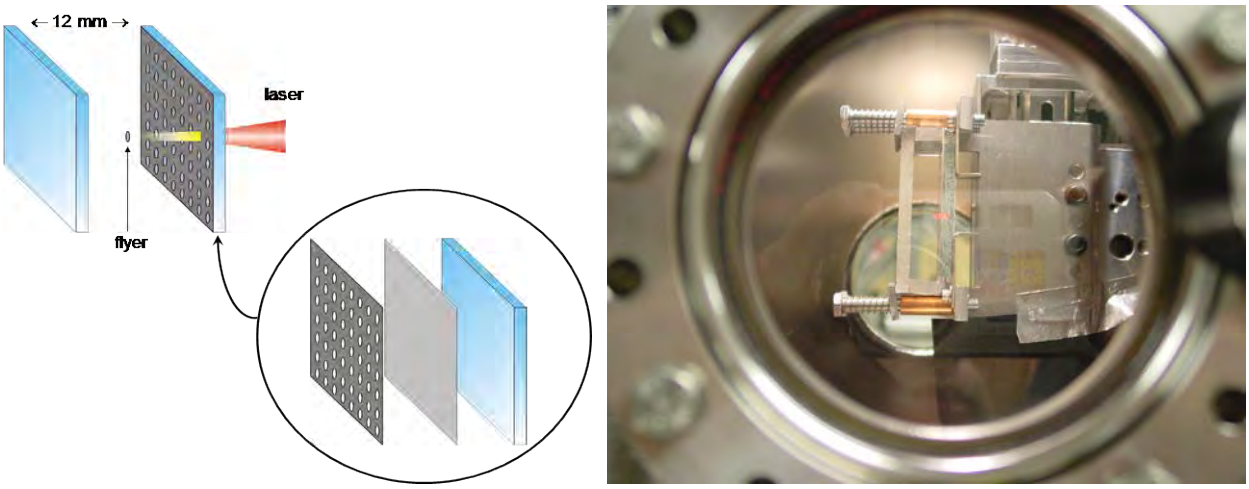


**Figure 16. Homemade sample coupon assembly & holder c2006**
*Right panel shows a side view through 6-inch Conflat port; laser would be incident from the right. [WL1065]*

Figure 16 shows the new sample coupon assembly we adopted to protect the "downstream" viewport, which uses a sacrificial glass or polymer "anvil" spaced ≈ 12 mm from the target. This design also incorporates a ≈ 600-μm-thick perforated steel mask to reduce the foil detachment and "petalling" caused by the expanding laser-driven plasma, which is evident in the left and middle panels of Figure 17. These "blisters" left from prior flyer launches must not be allowed to overlap the laser focus spot for a subsequent flyer, thus the size of the blisters sets the minimum spacing between flyer launch sites, and so too the number of flyers that can be produced from a single target.

As in the experiments depicted above in figure 15, the 13-μm-thick Ti foil cannot survive intact a flyer launch laser energy of 1.3 J; the resulting fragments can be seen in flight in the right panel of Figure 17. The glass anvil used in this experiment (not shown) exhibited a "shotgun pattern" of many small impacts, confirming the disintegration of the flyers. This result lent further motivation to our efforts to attenuate and control the delivered laser pulse energy.

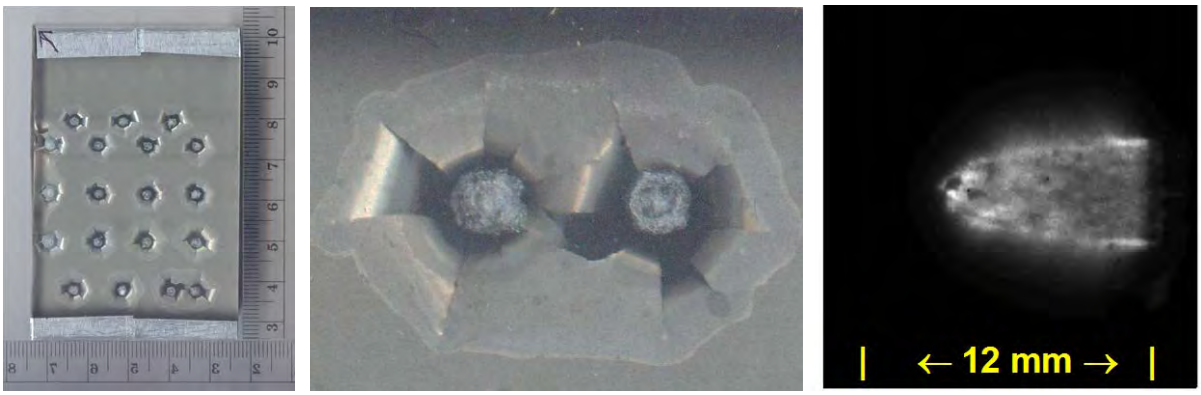


**Figure 17. 13 μm Ti foil without overlying steel mask**
*Ti foil glued to glass; $E_{laser}$ = 1.3 J, $d_{spot}$ = 3 mm, exposure = 50 ns, delay = 4 μs. [WL1070]*

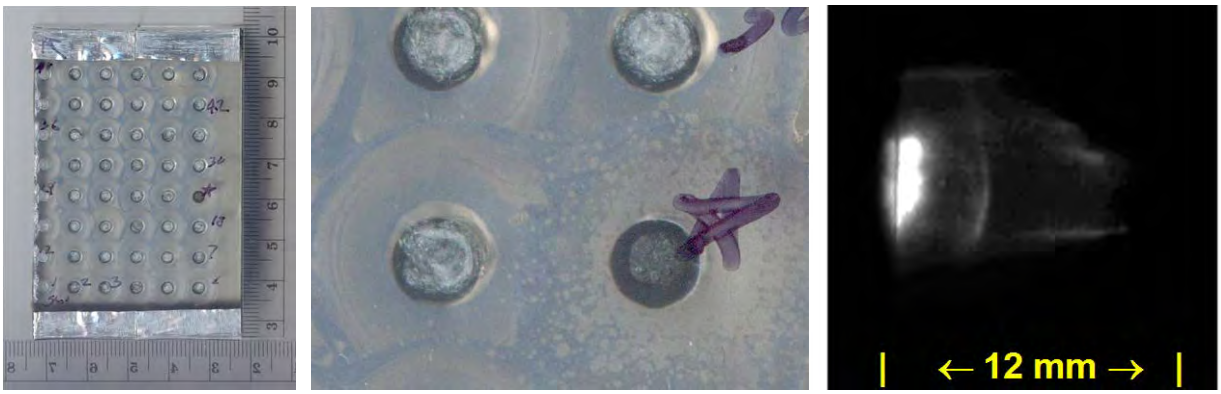


**Figure 18. 25 μm Ti foil with overlying 600 μm steel mask**
*Ti foil glued to glass; $E_{laser}$ = 1.3 J, $d_{spot}$ = 3 mm, exposure = 50 ns, delay = 12 μs. The star in the middle panel denotes a pre-existing air bubble in the epoxy layer. [WL1083]*

Our next experiments employed thicker and tougher metal flyer foils. Figure 18 shows the results from similar experiments using a 2x thicker titanium foil supported by an overlying 600-μm-thick perforated steel mask. As shown in the middle panel, the "blisters" from prior flyer launches do not extend to the laser focus spots for other flyers. The right panel in Figure 18 shows the impact luminescence recorded at a delay of 12 μs following the flyer driving laser pulse; also visible is the reflected shock running back into the flyer launch plasma gaseous debris. A typical impact time of t = 11 μs, at a target-to-anvil distance of 12 mm, translates to a velocity of $v_{flyer} \approx 1.1$ km/s. Assuming a nominal mass for the flyers of $m_{flyer} \approx 0.8$ mg, the flyer kinetic energy is $KE_{flyer} = ½\ m\ v^2 \approx 0.5$ J, which is roughly 40 percent of the incident laser energy. Figure 19 shows the distinct, individual impact marks left by the 25 μm Ti foil flyers, confirming that they arrive with far less fragmentation than the thinner 13 μm Ti foil flyers.

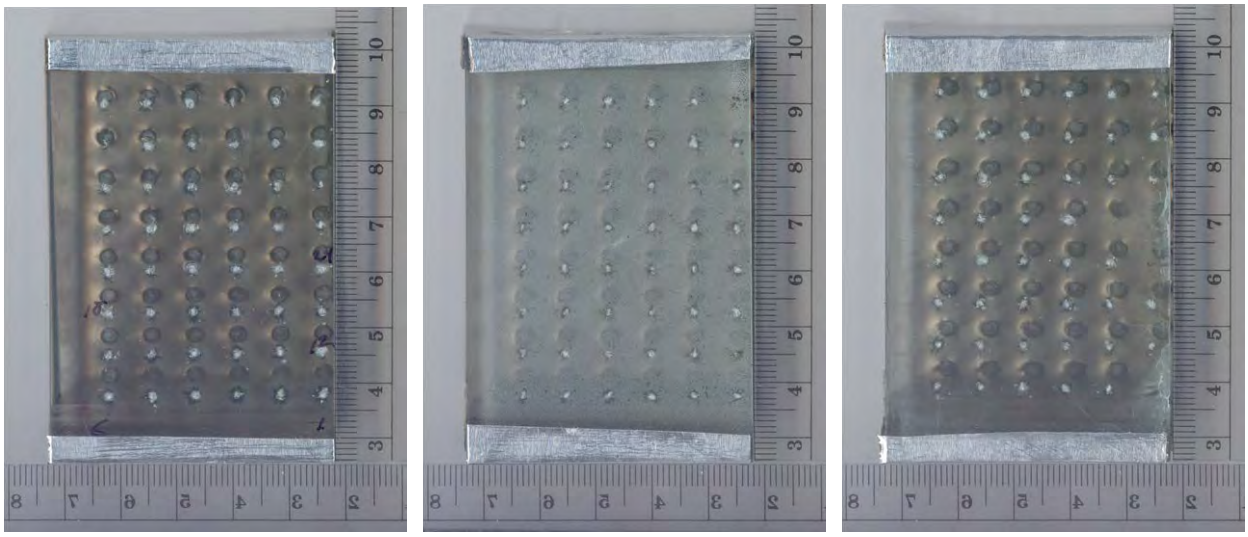

**Figure 19. Anvil impact marks left by 25 μm Ti foil flyers**
*Left - soda-lime glass, center - nanoAl/Teflon AF film on glass, right - nanoAl/PVC film on glass. [WL1095, WL1093, WL1089]*

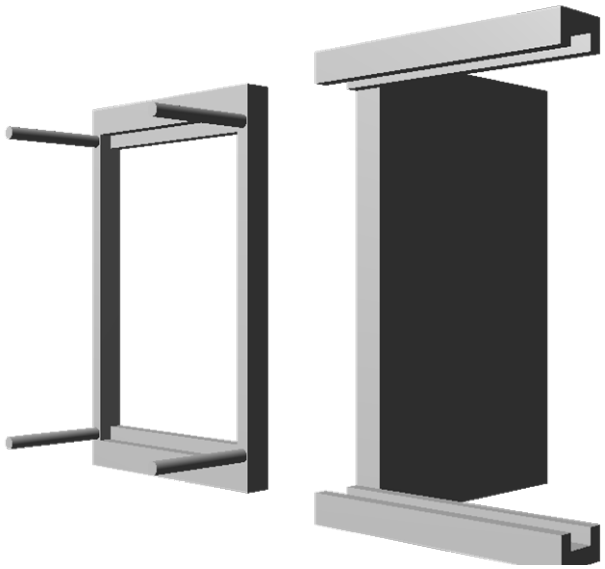

**Figure 20. Stainless steel sample coupon frame & holder c2007** *[WL2056]*

As can be seen in Figures 16-19, the experiments performed prior to July 2007 were accomplished using sample coupons assembled with epoxy adhesives and aluminum tape (MIL-T-23397B TYPE II). We eventually designed, and had constructed, a new stainless steel (SS) sample coupon frame and matching holder, as shown in Figure 20. The holder is attached permanently to the XYZ translator, and includes spring-loaded plungers that engage detents in the frames for reproducible positioning when changing samples. The shallow recess in the frame accommodates a 2x3x1/4 inch glass target. The protruding round posts are threaded near the ends and serve for stacking additional components, like the SS perforated mask shown in the right panel of Figure 21, in registration. We use tubular spacers captured on the round posts to separate the various layers of the assembled sample coupons.

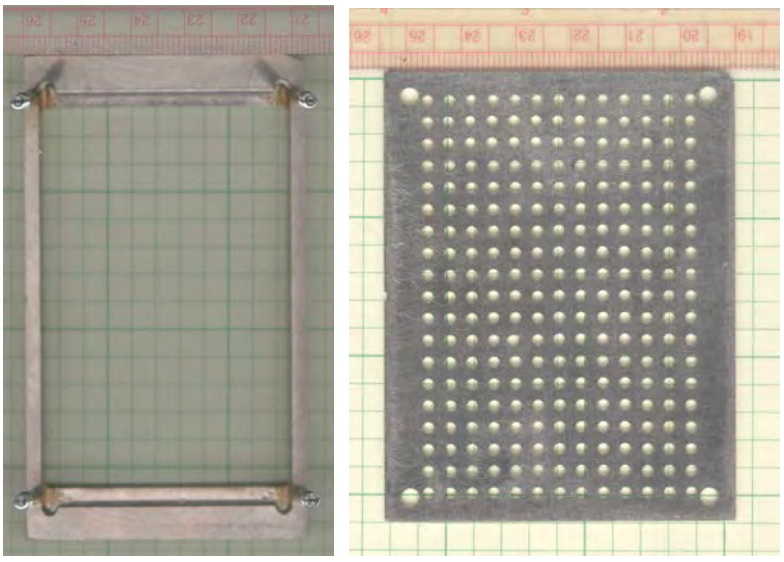

**Figure 21. Stainless steel sample coupon frame & perforated mask c2007** *[WL2056]*

### 3.C. Energetic Material Sample Preparation

#### 3.C.1 Spin Coating of Energetic Thin Films

Our first efforts at producing energetic materials samples employed a commercial spin-coater, which mounts the horizontal sample substrate balanced on a rotatable "chuck." A drop of energetic material solution is placed at the center of the substrate, and the substrate spun at a programmed sequence of angular velocities optimized to yield a uniform coating of the desired thickness. We produced thin films of nanoAl/PVC and nanoAl/Teflon AF on glass substrates (see Figure 19), as well as pure nitrocellulose films on Al metal plate, Al coated mirror, and SS foil substrates. We continue to use this approach routinely to the present day, but have made no advances to the state-of-the-art worth reporting.

#### 3.C.2 Drop Casting of Energetic Material Solutions

Most of our samples to date were produced by "drop casting," *i.e.* drop-wise deposition and evaporation, of an energetic material dissolved in a volatile organic solvent, such as pentraerithritol tetranitrate (PETN) in acetone. Our earliest samples were hand-pipetted as individual drops onto the sample substrates. To improve both the quantity and quality (reproducibility) of the samples, we acquired and reprogrammed an automated liquid handler originally designed for filling racks of test tubes, as shown in Figure 22. In this case, a drop of solution is delivered into each of the individual "wells" formed by stacking a perforated mask atop the sample substrate. We encountered a number of problems while working with these pre-assembled target coupons. Most significantly, we noticed considerable "wicking" of the solution into the thin gaps between the perforated mask and the substrate, resulting in trapped solid deposits which might be crushed during shock loading of the assembly.

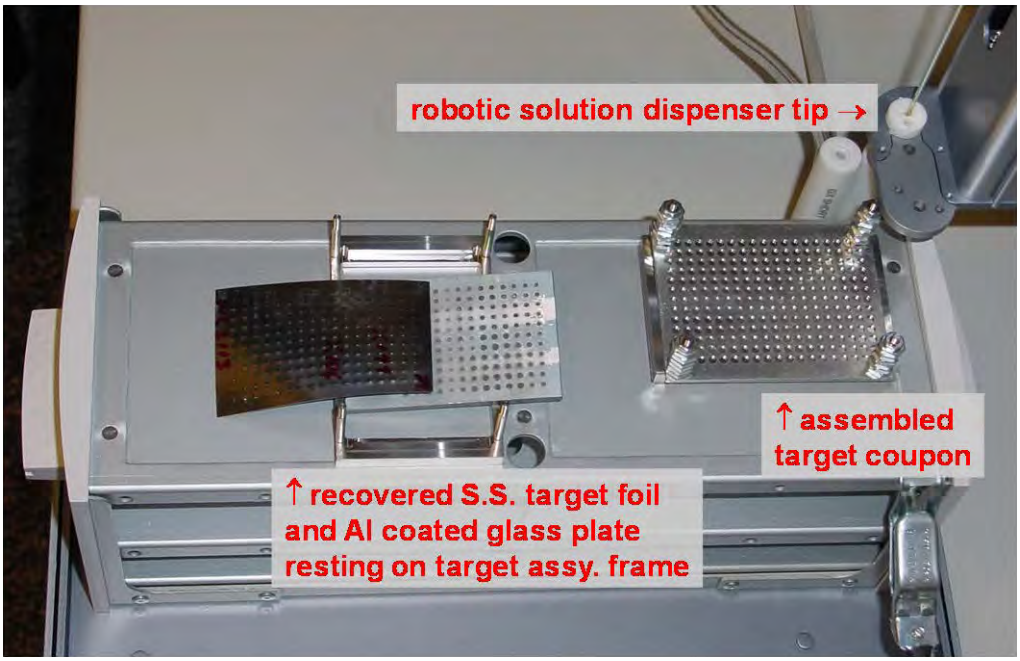


**Figure 22. Automated liquid handler & sample coupon components** *[WL2062]*

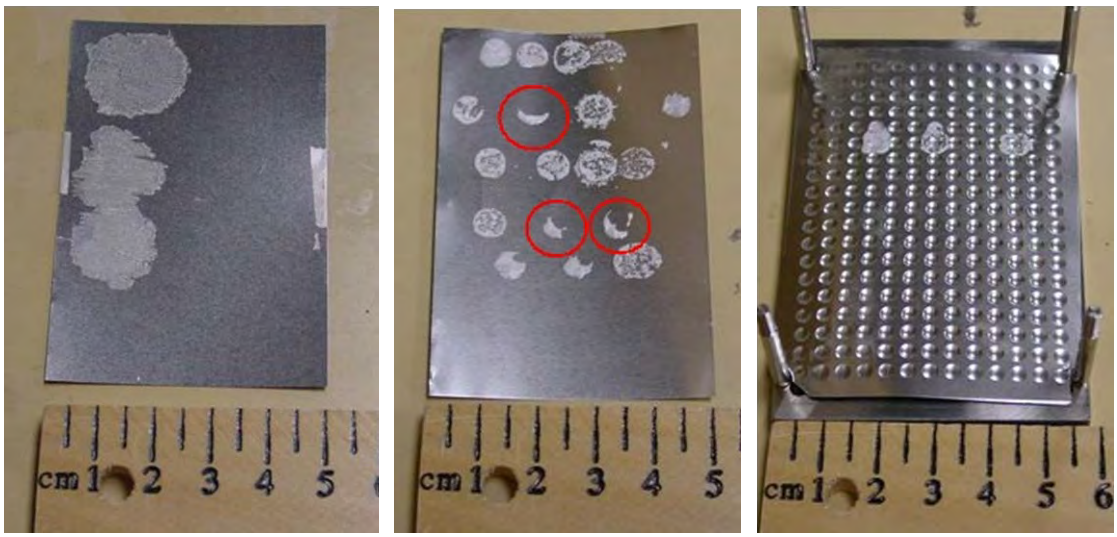


**Figure 23. Drop casting aspirin on stainless steel foil**
*Each spot is the residue from a 10μL drop of 90% saturated aspirin/acetone solution. [RN1015]*

We subsequently turned to drop casting individual spots onto unassembled substrates, as shown in Figure 23. The left and center panels show the variation in spreading of the solution encountered due to the surface finish of different SS foils. The smaller spots in the center panel show extreme examples of the "coffee ring stain effect," in which capillary flow during evaporation leads to non-uniform solid deposits [94]. The right panel shows that wetting of the substrate by the solution can easily overcome gravitational forces, resulting in spreading beyond dimples pressed in the SS foil. We attempted to mitigate these problems, with mixed results, by: depositing smaller drops, varying the solute concentration, varying the deposition temperature, and cleaning/modifying the substrate. As shown in Figure 24, we were able to produce ≈ 1-mm-diameter PETN sample spots by drop casting an acetone solution onto a glass plate; however the inhomogeneous sample morphology still leaves much to be desired.

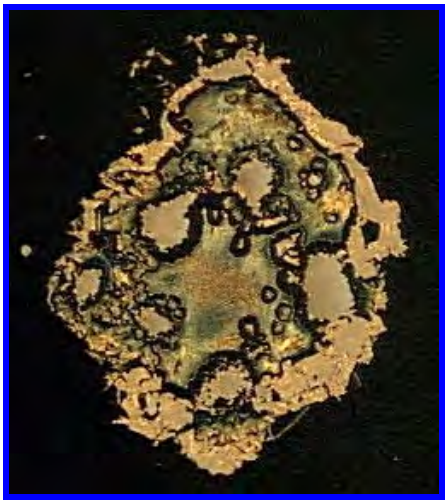

**Figure 24. Drop casting PETN onto a soda-lime glass plate**
*The spot is roughly 1.0x1.2 mm. [CM04139]*

### 3.C.3 Spray Deposition of Energetic Material Solutions

We briefly considered purchasing a commercial chemical inkjet printer, but abandoned this alternative when we learned the system would not satisfy even a ~ 1 μg/s solute mass throughput requirement. Spray deposition with a hand-held airbrush had been used successfully to produce uniform polycrystalline thin films in some of the ultrafast laser experiments cited in the Proposal [59-61]. Figure 25 shows a sample we made by hand-spraying an aspirin/acetone solution onto SS foil taped to a perforated SS mask with 3-mm-diameter clear holes. The optical micrograph suggests that the small droplets evaporate quickly leaving a dense sintered polycrystalline mass.

Figure 26 shows our home-made automated spray-coating system that rasters a masked deposition substrate beneath a fixed airbrush source. The overspray is contained within a plastic tub (not shown) which is secured to the XY-table by small magnets, and which makes a slide seal against the transparent plastic plate. We have demonstrated the production of well-defined sample spots, with good adhesion to flexible SS foil substrates, by spraying aspirin/acetone solutions. We are pursuing safety approval to proceed with PETN/acetone spray depositions.

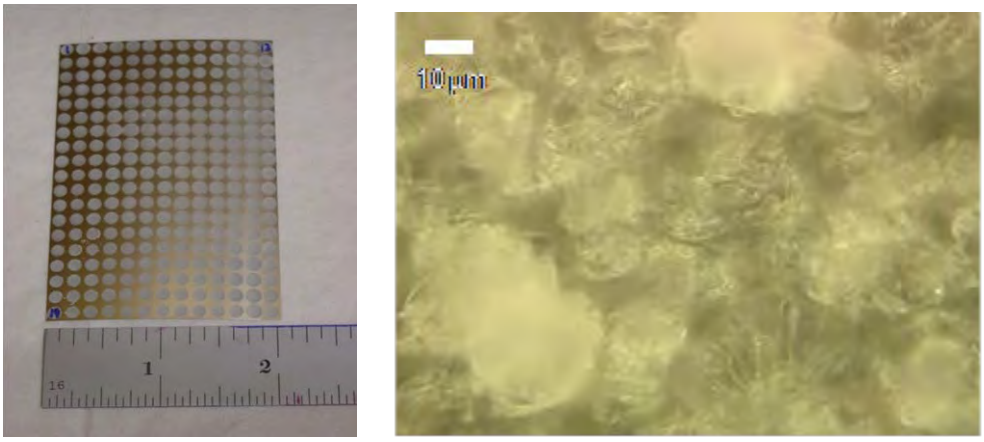


**Figure 25. Spray deposition of aspirin on stainless steel foil** *[RN1023, CM04059]*

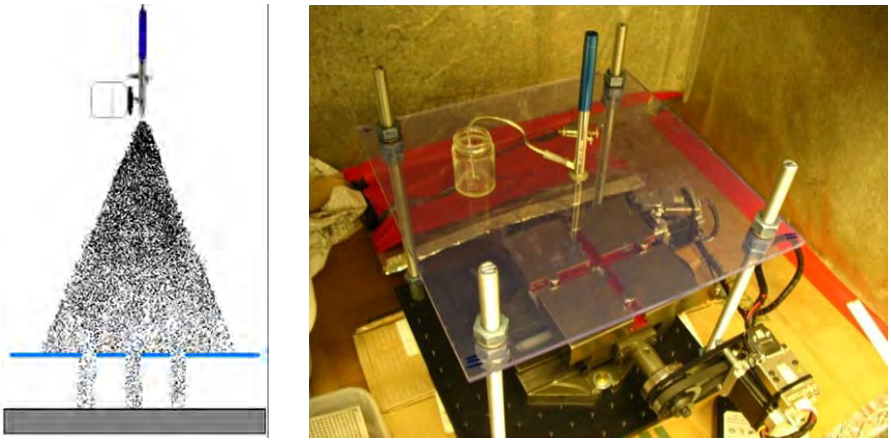

**Figure 26. Automated spray deposition apparatus** *[RN1029]*

### 3.D. Photographic and Spectroscopic Diagnostics

#### 3.D.1 Photographic Flyer Velocity Measurements

Figure 27 shows IgCCD camera images of ten consecutive flyers launched from the 25 μm Ti foil sample depicted above in Figure 18. These images show some flyer fragmentation and tilting, but not as much as observed for the 13 μm Ti foil flyer "shotgun spray." From these images we calculate the flyer velocity as distance travelled divided by the 9 μs delay time. The single outlier velocity of 0.85 km/s (marked by the asterisk) corresponds to the spot overlapping a pre-existing air bubble in the epoxy layer. Including this low velocity value yields an average flyer velocity of $v_{flyer}$ = 1.07(0.09) km/s, where the value in parenthesis is the standard deviation over the ten shots. Excluding the air-bubble value yields $v_{flyer}$ = 1.10(0.05) km/s. These results show that, with proper quality control of our substrates, we can expect fairly reproducible flyer velocities with standard deviations of 10 percent, or substantially less.

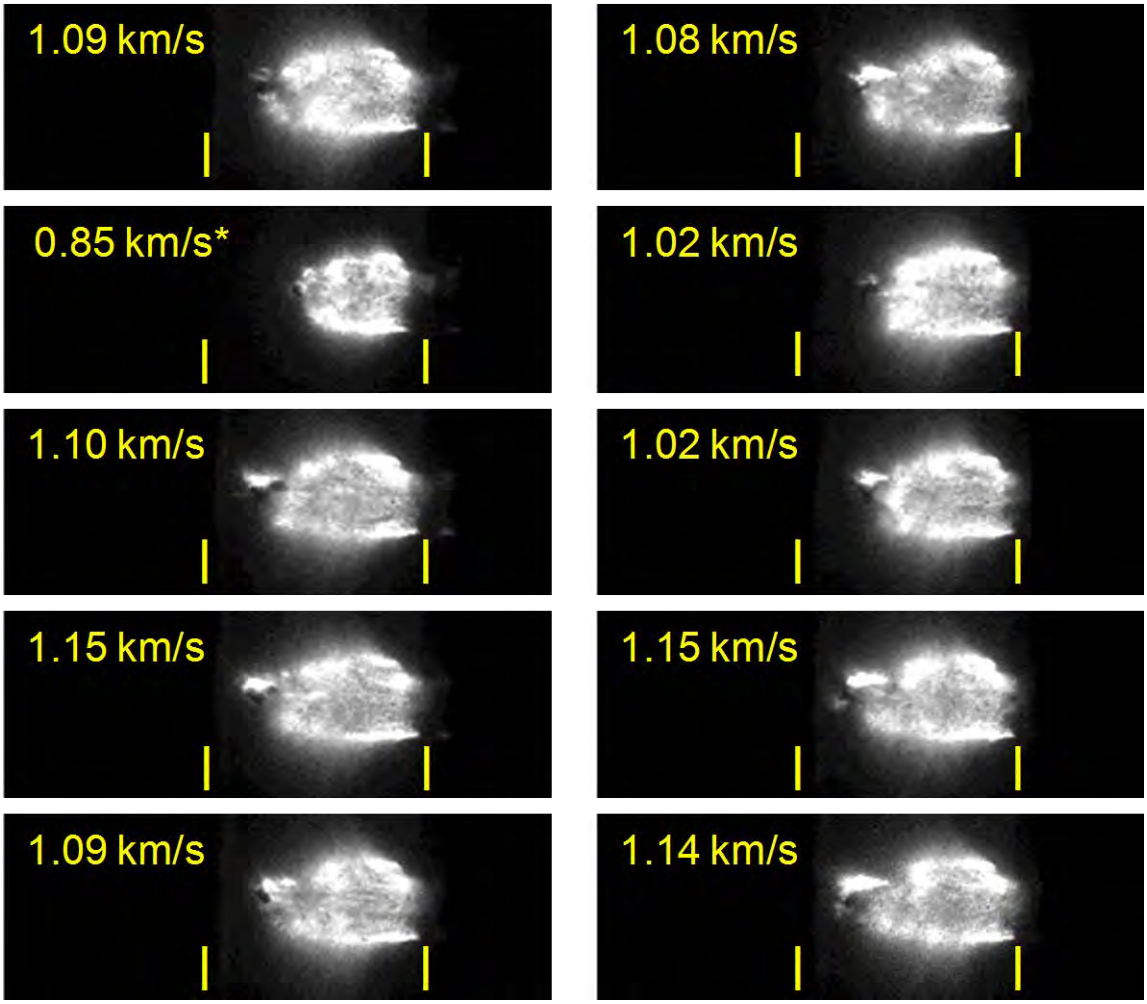


**Figure 27. Flyer velocity reproducibility**

*25 μm Ti foil glued to glass; $E_{laser}$ = 1.3 J, $d_{spot}$ = 3 mm, exposure = 50 ns, delay = 9 μs. Same sample as in figure 18. The vertical yellow lines are spaced by 12 mm. [WL1083]*

### 3.D.2 Impact Luminescence Flyer Velocity Measurements

Figure 28 shows the flyer launch and impact process viewed through a transparent glass anvil. The first image, taken at a delay of t = 3 μs, shows the breakout of the flyer driving plasma around a satisfyingly round central dark spot, which we take to be the shadow of the flyer. The images at t = 7 & 10 μs also show a single, fairly round, dark central shadow. The image at t = 11 μs shows a sudden increase in luminosity which we attribute to the impact of the flyer on the transparent glass anvil. These observations suggested the flyer velocity measurement scheme shown in Figure 29. We added a fiber optic feed-through to the main vacuum chamber, and positioned the end of a large diameter (600 μm) optical fiber a few millimeters behind the transparent glass anvil. This fiber runs to a fast silicon photodiode with a 1 ns rise time, which is monitored by a 1 GHz analog bandwidth oscilloscope.

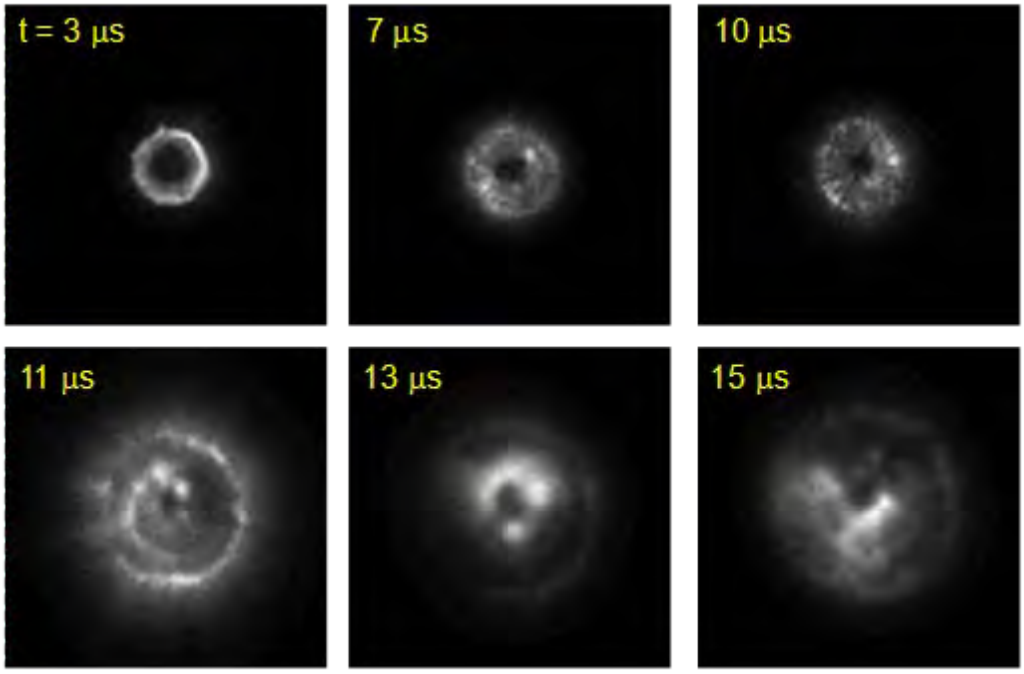


**Figure 28. Impact luminescence as seen through transparent anvil**
*25 μm Ti foil glued to glass; $E_{laser}$ = 1.3 J, $d_{spot}$ = 3 mm, exposure = 50 ns. [WL1079]*

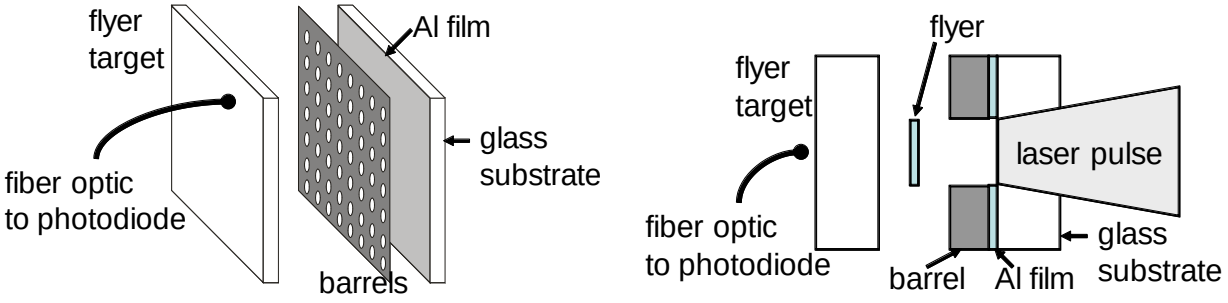


**Figure 29. Fiber optic impact luminescence probe**

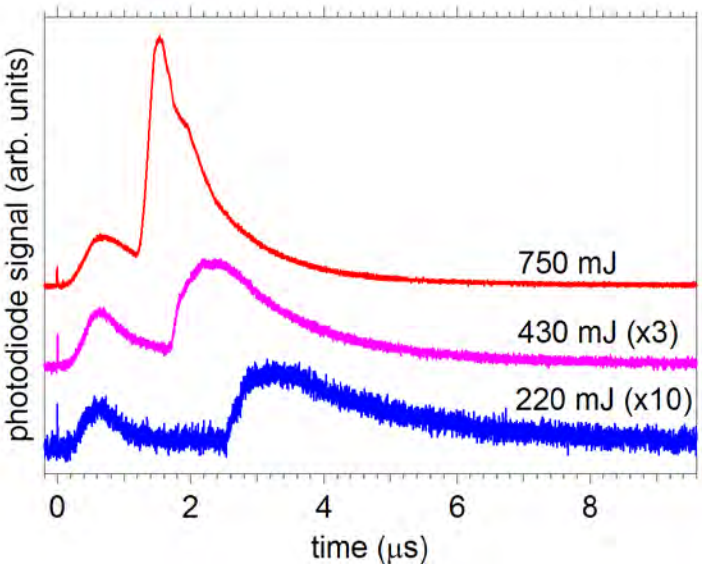


**Figure 30. Photodiode traces of Al flyer impact luminescence**
*10 μm physical vapor deposited (PVD) Al film on glass; 7.3 mm anvil standoff. [WL2098]*

Figure 30 shows the photodiode traces revealing the scattered 1064 nm laser light (sharp spike at zero time), the laser-driven plasma light breakout (first subsequent peak), and the anvil impact luminescence (last peak). For these measurements, the laser was focused to a 3-mm-diameter spot, and the glass anvil was spaced 7.3 mm from the sample substrate. Figure 31 shows a comparison of the measured flyer velocities obtained by this method using a 10-μm-thick physical vapor deposited (PVD) Al film and a 10-μm-thick piece of Al foil glued to the glass substrate. Both methods yield flyer velocities over the 1-5 km/s range, and an overall conversion efficiency of laser pulse energy to flyer kinetic energy of ≈ 30 percent.

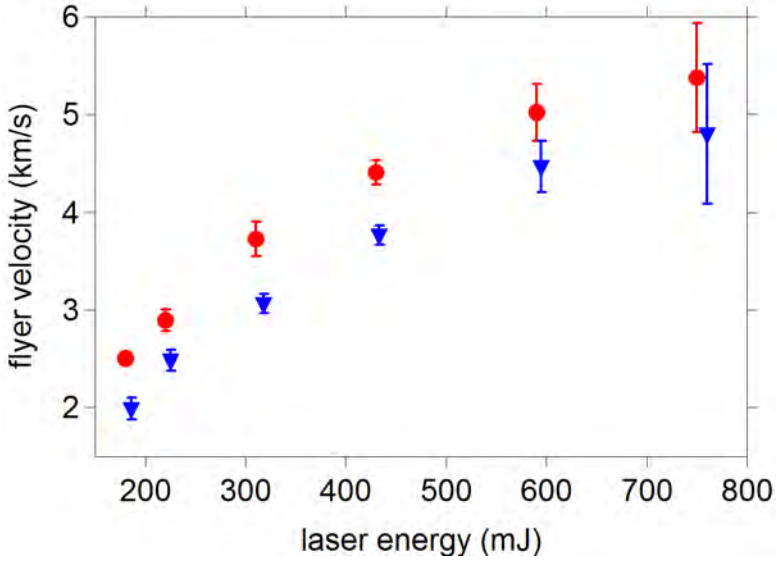


**Figure 31. Flyer velocity *vs.* laser energy**
*PVD 10 μm Al film on glass (red) and 10 μm Al foil glued to glass (blue). [WL2098, WL2119]*

### 3.D.3 Emission Spectroscopy Diagnostic

As indicated in the Proposal, we had high hopes of applying emission spectroscopic diagnostics to learn about the chemical kinetics of reacting energetic materials in vacuum. Thus, we began early on to record spectra of luminous events using a miniature fiber-optic coupled grating spectrometer, and a spectrometer comprised of the IgCCD camera mounted onto a 0.3 m focal length tunable monochromator. Figures 32 and 33 show time-integrated spectra of various laser-driven events recorded with the miniature fiber-coupled spectrometer. The spectra point to the effectiveness of the focused laser beam in exciting many strong and sharp emission features, which may interfere with measurements of light emitted by reacting energetic materials.

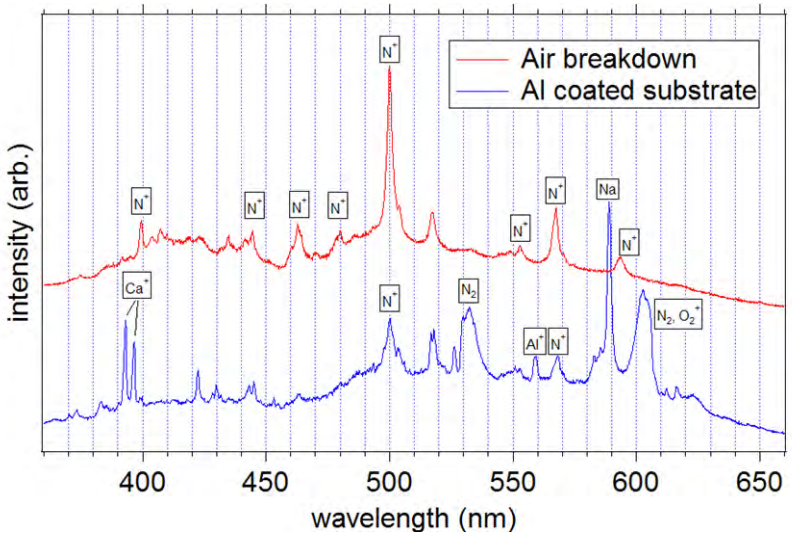


**Figure 32. Emission spectra of dielectric breakdown in air and above an Al mirror**
*[WL1052]*

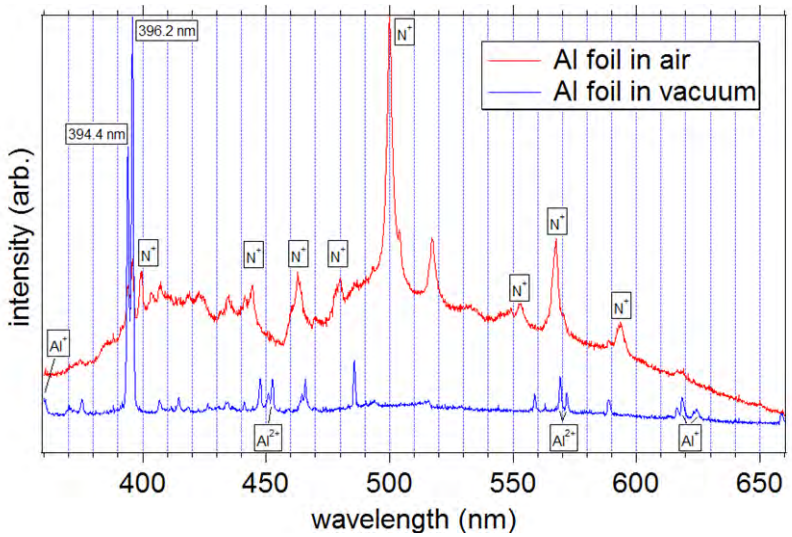


**Figure 33. Laser ablation emission spectra, Al foil in air and under vacuum**
*Note strong Al atomic emissions at 394.4 and 396.2 nm. [WL1059]*

### 3.D.4 Time-Resolved Impact Luminescence Spectroscopy

One approach to reducing potential spectroscopic interference from the initial laser-driving process is to make time-resolved spectral measurements, employing delay times well after the laser-driven plasma emissions have decayed. Figure 34 shows a series of such spectra recorded during the launch and impact of Ti flyers produced from 25 μm Ti foil glued to a soda-lime glass substrate. Strong Ti atom emissions from the flyer-driving plasma are apparent at early times. The flyer impact at t ≈ 11 μs is once again accompanied by an increase in luminosity, as seen above in Figures 18 and 28, which persists on a timescale of ~ 10 μs.

The origin of this luminosity is puzzling. For Ti impacting soda-lime glass at a velocity of 1.1 km/s, we calculate a peak shock pressure of $P_{max} \approx 45$ kbar using the "impedance matching" method [40]. The irreversible shock-induced heating of the glass substrate should amount to 10-100 K, far below the temperatures required for visible blackbody emission. It may be that the flyer traps and compresses some of the remnant gases from the flyer driving plasma that "blow-by" the flyer and reach the anvil first. Figure 18 clearly shows a shock front running back into these remnant gases, and we have repeated this observation a number of times in this sample coupon geometry. The timescale for shock reverberation in the remnant gases between the sample substrate and anvil is of the same order of magnitude as the persistent luminosity, so shock re-heated gas is our most likely candidate emitter. Figures 35 and 36 show that a blackbody fit to this unstructured broadband emission yields a temperature estimate of ≈ 3000 K.

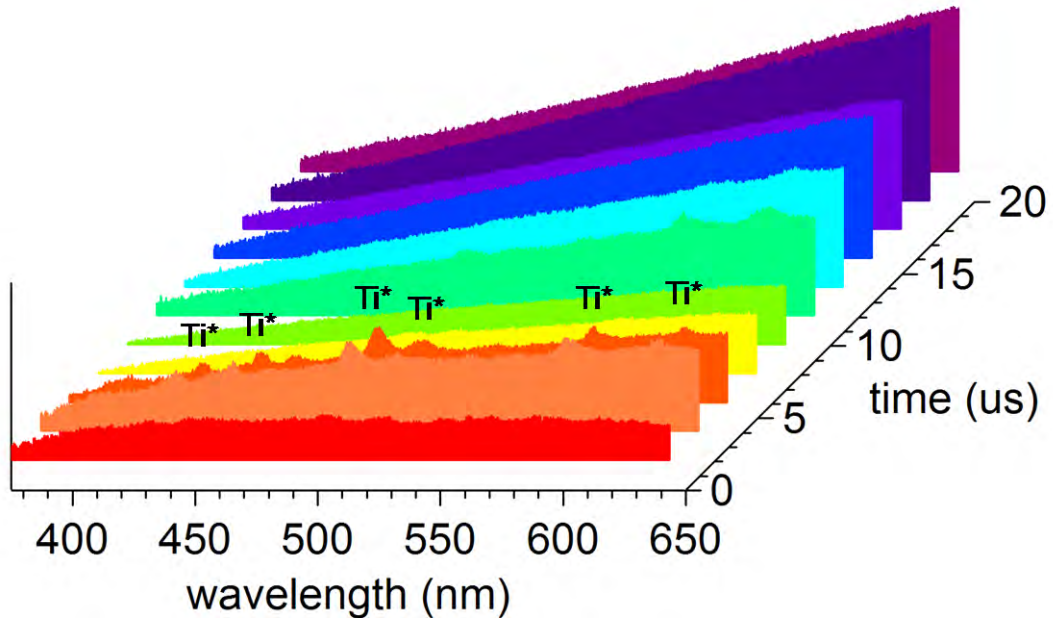


**Figure 34. Time-resolved impact luminescence spectra**
*Nominally 25 μm Ti flyer impacting PMMA at 1.1 km/s;*
*$E_{laser}$ = 1.3 J, $d_{spot}$ = 3 mm, 50 ns exposures. [WL1085]*

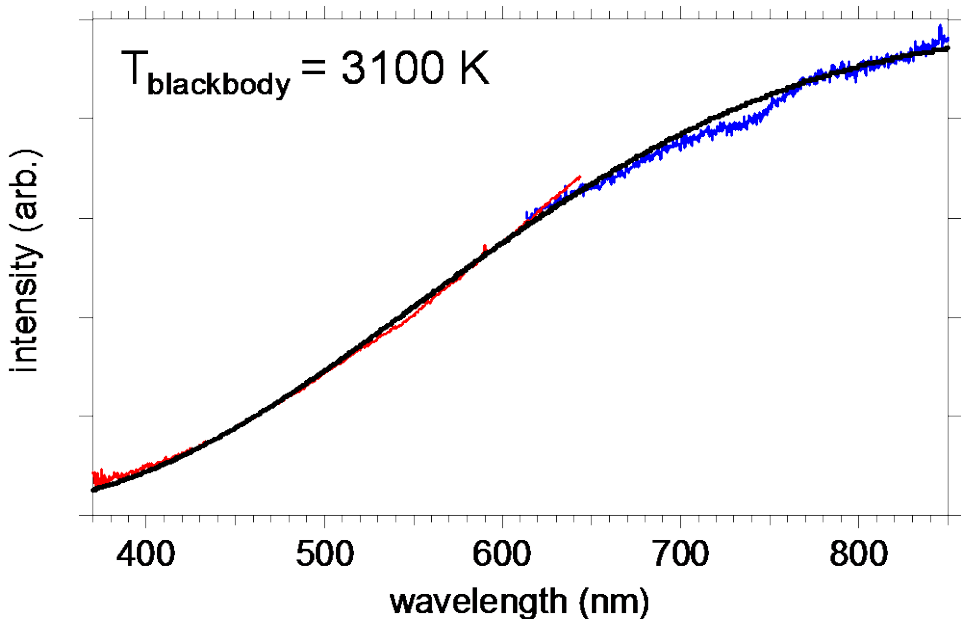


**Figure 35. Ti/glass impact luminescence spectrum**
*Nominally 25 μm Ti flyer impacting soda-lime glass at 1.1 km/s; delay = 8 μs, exposure = 50 μs. [WL1095]*

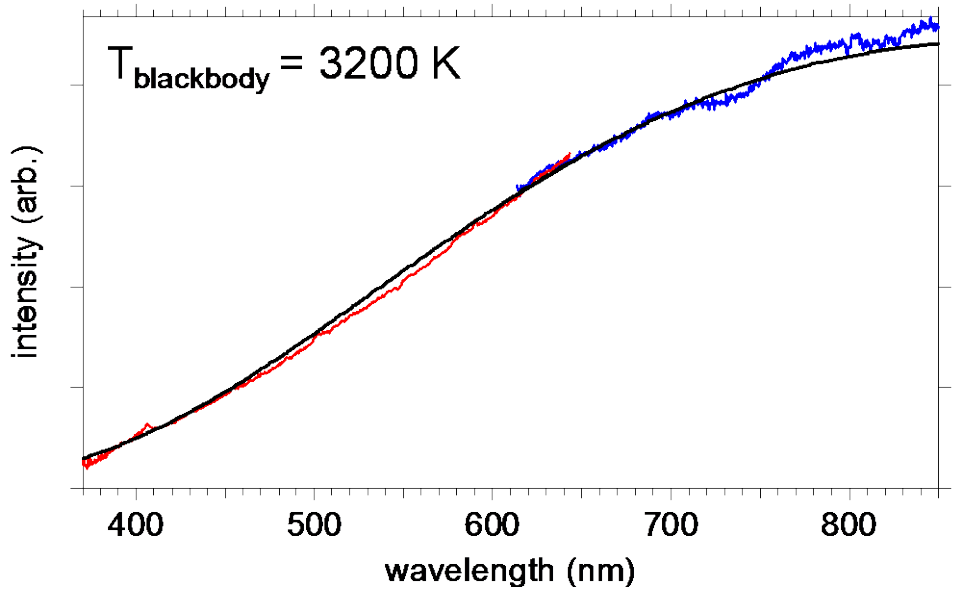


**Figure 36. Ti/(nanoAl+Teflon AF)/glass impact luminescence spectrum**
*Nominally 25 μm Ti flyer impacting nanoAl/Teflon AF coating on soda-lime glass at 1.1 km/s; delay = 8 μs, exposure = 50 μs. [WL1095]*

### 3.E. Mass Spectrometric Diagnostics

#### 3.E.1 1st Generation TOFMS Experiment

The absence of distinct, assignable spectral features in the flyer impact emission spectra shown above in Figures 34-36, even on anvils coated with energetic materials -- along with the problem of spectral interference from the laser plasma and its remnant gases -- encouraged us to move away from spectroscopic diagnostics and towards time-of-flight mass spectrometry (TOFMS). In so doing, we took on the closely related problem of interference by the laser driven plasma gaseous products with the TOFMS measurements.

Fortunately, a very clever sample configuration was reported by Buelow and coworkers in which these gaseous products are trapped behind an intermediate metal foil barrier [95], as shown in the lower right corner of Figure 37. In this arrangement, the laser driven flyer impacts the enclosed side of a thin metal foil, the exposed side of which is coated with the energetic material sample. The shock from the flyer impact transits the metal foil and ignites the energetic material. Our adaptation combines Buelow's target configuration with Dlott's "nanoshock target array" approach [54-63] for producing repetitive events. An example of a recovered foil barrier can be seen resting atop its companion flyer launch substrate in Figure 22.

As suggested by the cartoon in Figure 37, in our 1st generation mass spectrometry apparatus the TOFMS diagnostic was simply bolted onto the main vacuum chamber at the "downstream" 6-inch Conflat port. A flat metal plate with a 6-mm-diameter hole aligned with the line-of-sight between the laser focus and the ionization region of the TOFMS served to limit the gas conductance between the two chambers. Also shown in Figure 37 is the location of a fast ionization gauge (FIG), with a ~ 1 μs response time, which proved very helpful in determining the arrival times of the gaseous products from the reacting energetic material samples.

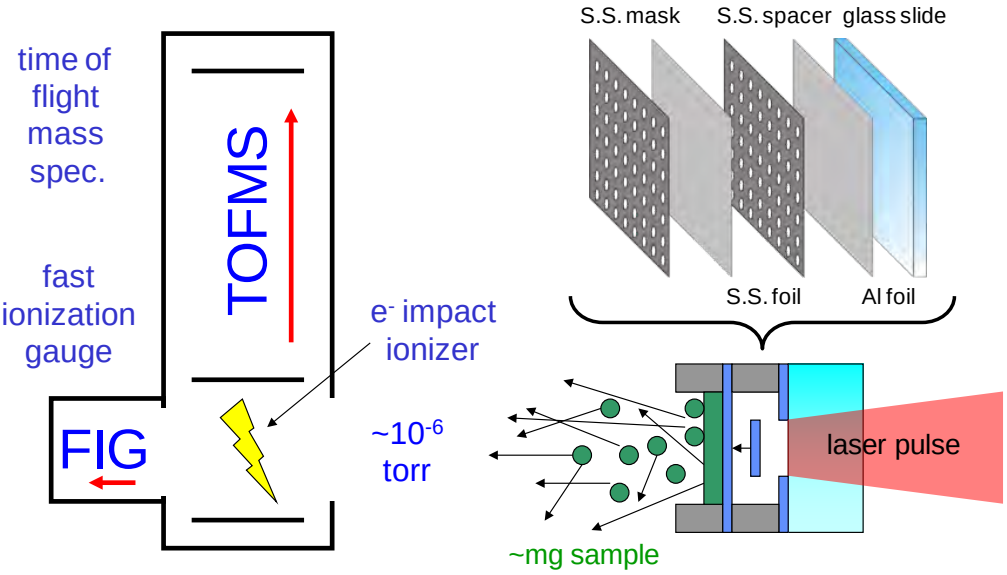


**Figure 37. 1st generation TOFMS experiment c2007**
*Laser incident from the right. [WL1105]*

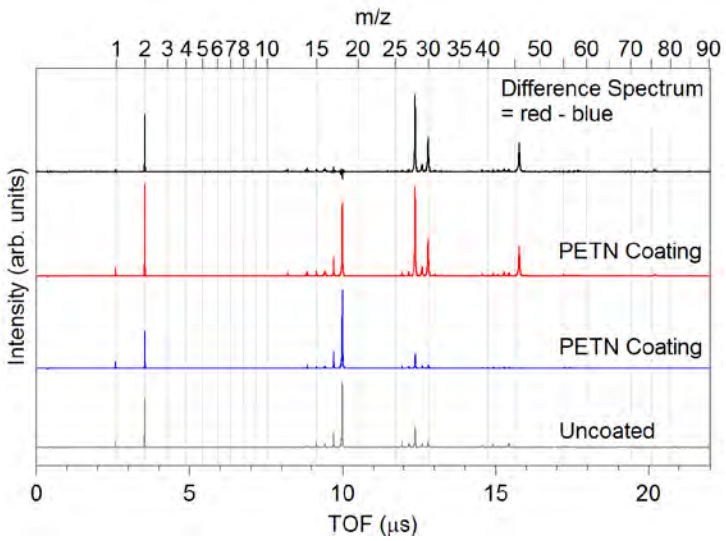


**Figure 38. TOFMS data from shocked PETN samples reacting in vacuum**
*Average of 40 scans acquired at a 20 kHz repetition rate. [WL2071, WL2077]*

We reported several results obtained from drop-cast PETN samples using this experimental configuration in ref. [89]. Briefly: as shown in Figure 38, we observe primarily those gaseous products consistent with the in-vacuum deflagration of PETN [96]: CO (or $N_2$) at m/z = 28, NO (or CHO) at m/z = 30, and $NO_2$ at m/z = 46. We specifically do not observe any thermodynamically stable detonation products ($H_2O$, $CO_2$). The images in Figure 39, taken using long IgCCD exposures, show burning PETN particles emanating from the sample spot with velocities ~ 1-10 m/s. The FIG traces showed a rise-time ~ 100 ms, which is consistent with slow gas production by the self-propelled burning PETN particles. Even for air molecules ($N_2$, $O_2$), with room temperature molecular velocities ~ 500 m/s, the timescale for crossing the 0.5-m-diameter main vacuum chamber is only ~ 1 ms. Thus, the ~ 100 ms FIG signal risetime suggests a strong detection bias for chemically stable and volatile products capable of reaching the TOFMS ionization region after surviving multiple collisions with the main chamber walls.

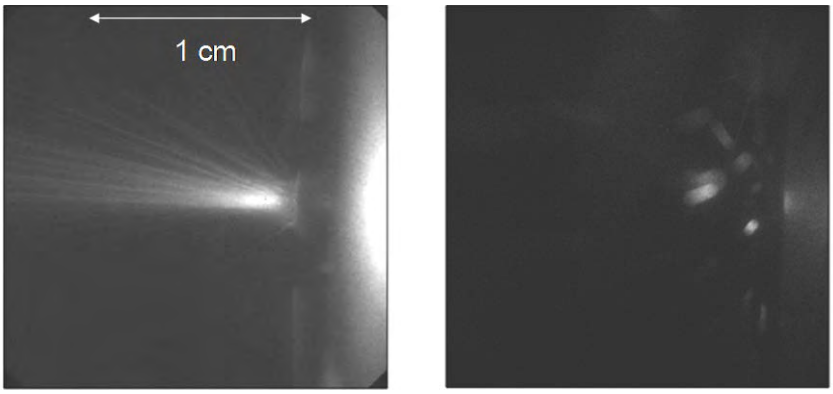


**Figure 39. Images of shocked PETN samples reacting in vacuum**
*Left: 50 μs delay, 25 ms exposure. Right: 7 ms delay, 1 ms exposure. [WL2018]*

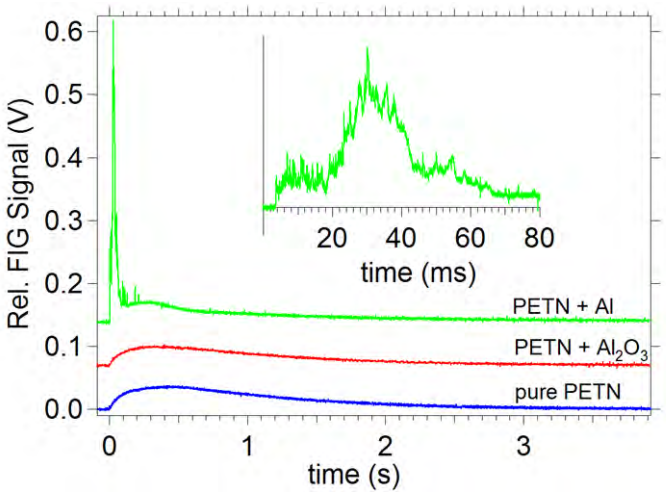


**Figure 40. Effect of nanoAl on gas production rate of shocked PETN samples**
*[WL2063, WL2087, WL2113]*

Despite these limitations, we were able to obtain some intriguing preliminary results on drop-cast PETN samples containing ≈ 25 percent by weight 50 nm Al, or 50 nm $Al_2O_3$, particles. Figure 40 shows similar ~ 100 ms FIG signal risetimes for the pure PETN and nano$Al_2O_3$/PETN samples, but early-time pressure spikes with ~ 10 ms risetimes for the nanoAl/PETN sample. The TOFMS data in Figure 41 shows that adding nanoAl reduces the CO and $H_2$ peaks, doesn't change the NO and $NO_2$ peaks, enhances the CHO peaks, and introduces several new peaks in the m/z = 39-45 region. In contrast, adding the supposedly chemically inert nano$Al_2O_3$ reduces the amount of NO and $NO_2$ produced and leads to the first observation of $CO_2$ at m/z = 44. We are still trying to make sense of these observations, and hope that the apparatus modifications described in the next section will prove helpful in that regard.

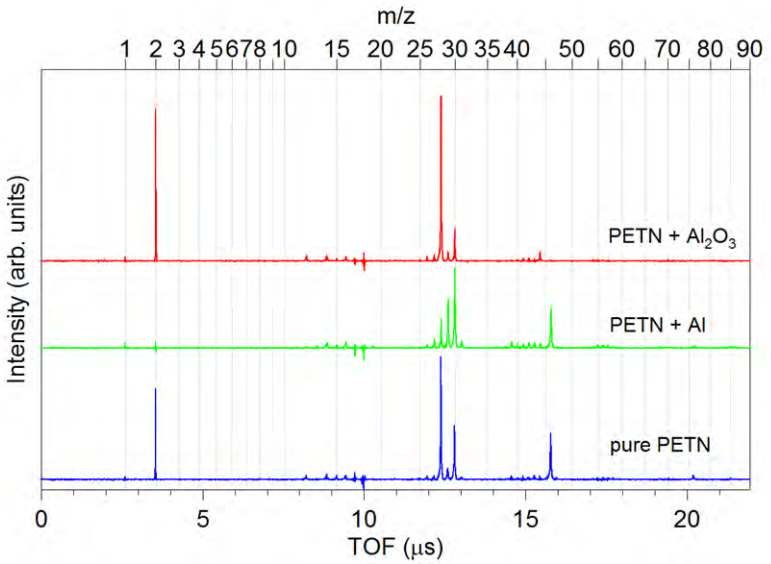


**Figure 41. Effect of nanoAl on PETN reaction products in vacuum**
*[WL2071, WL2083, WL2113]*

### 3.E.2 2nd Generation TOFMS Experiment

After completing the experiments performed with the 1st generation TOFMS apparatus, we re-evaluated our requirements for a useful TOFMS diagnostic. Certainly, we wanted to reduce the detection bias towards chemically stable reaction products that could reach the TOFMS ionization region after rattling around repeatedly inside the main chamber. Ideally, we would produce a collimated "molecular beam" from the reaction products; one whose composition would remain unaltered from that frozen in immediately following the initial expansion into vacuum. These considerations drove us to incorporate a differential pumping region between the main and TOFMS vacuum chambers, as shown in Figure 42. This is the approach adopted by the inventors of Los Alamos National Laboratory's (LANL's) physically much larger "Detonation Chemistry Apparatus" (DCA), which preceded our efforts by more than a decade [97, 98]. We became aware of the DCA when we started researching a mass spectrometric diagnostic, and had initially hoped (incorrectly) that the lower gas loads from our much smaller energetic materials samples would allow us to work with the simpler "bolt-on" TOFMS configuration.

The line-of-sight between the reacting sample spot and the TOFMS detection region is now defined by a pair of conical "skimmers" with 2-mm-diameter apertures. The skimmers are mounted on re-entrant cones to extend the time before the molecular beam can be perturbed by collisions with gas molecules reflected from the chamber walls. The differential pumping chamber is evacuated by four 50 L/s turbopumps (38-mm-diameter inlets) mounted radially around the chamber circumference. Any gas molecule entering this region at an odd angle is presented with ≈ 4500 $mm^2$ of area leading into the turbopumps, compared with ≈ 3 $mm^2$ of skimmer aperture leading into the TOFMS chamber. Gas molecules with trajectories originating elsewhere than the energetic material sample spot thus find it more than 1000 times more difficult to reach the TOFMS ionization region than before the apparatus modification.

Figure 42 also shows the addition of a second 500 L/s turbopump to the main chamber, which decreases the base pressure down to the mid-$10^{-7}$ torr range, as well as decreasing the pumpdown time following each energetic event.

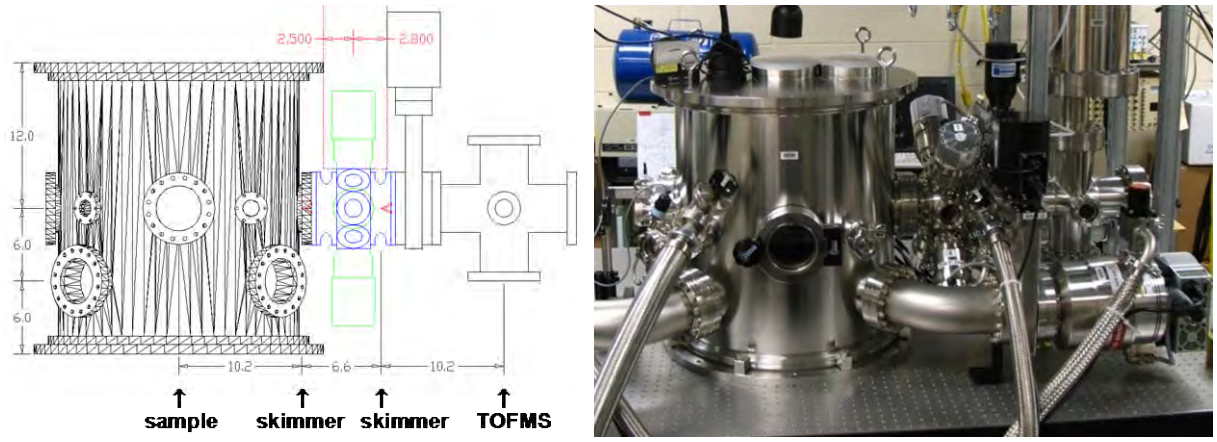


**Figure 42. 2nd generation TOFMS experiment with differential pumping c2009**
*Laser incident from the left. [MF11127]*

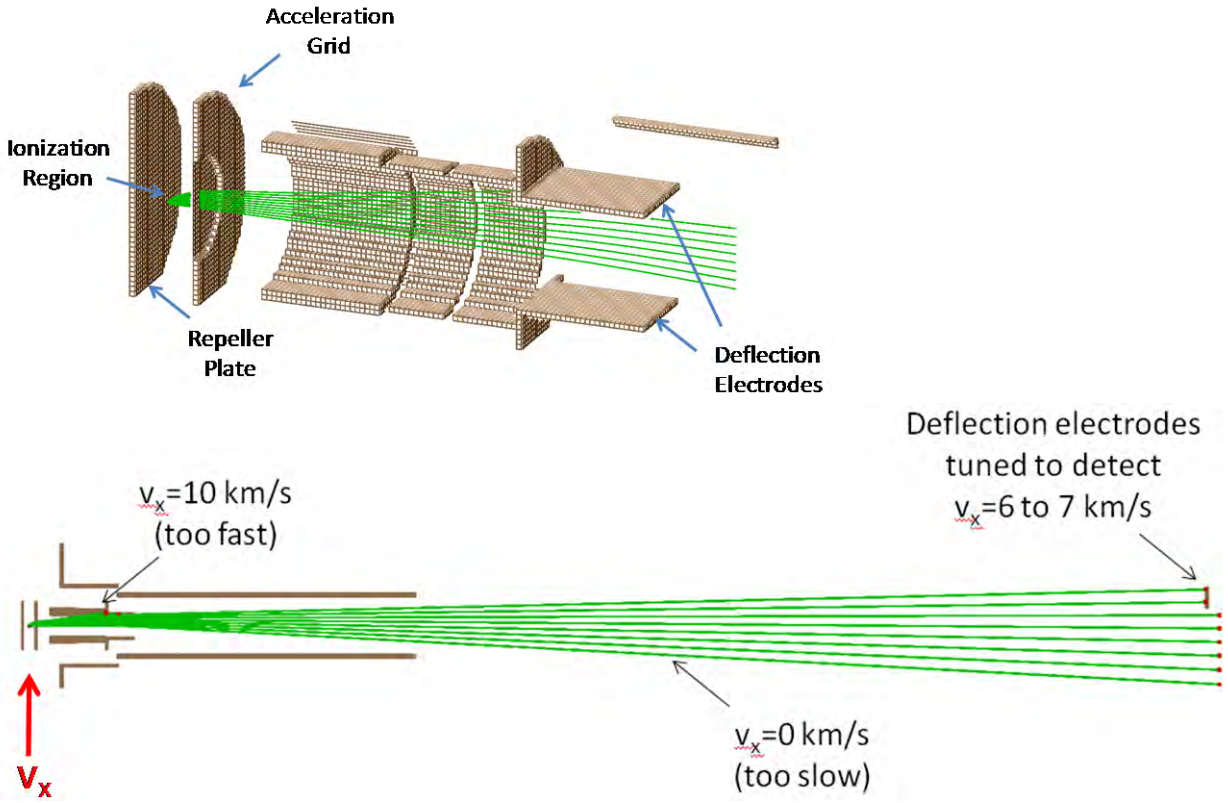


**Figure 43. Ion trajectories in TOFMS *vs*. neutral atom transverse velocities**
*Trajectories calculated using SIMION software package.*

The original manuscript describing the DCA [97] also included a discussion of how hyperthermal (v > 10 km/s) molecular species are produced when a detonation wave terminates at a free surface of a solid explosive in vacuum. This lead us to propose a novel chemically based diagnostic for distinguishing between an explosive deflagrating *vs*. detonating in vacuum: deflagrations produce quenched reaction intermediates with slower molecular velocities commensurate with the flame temperature, whereas detonations produce thermodynamically stable final reaction products with hyperthermal molecular velocities [89-91].

The challenge then became to demonstrate the detection of hyperthermal molecular species, and furthermore, to determine quantitatively their relative concentrations and velocity distributions. As discussed first in ref. [97], and illustrated in Figure 43, the requirement to detect both thermal and hyperthermal velocities greatly complicates the measurement scheme. In our TOFMS apparatus, ions are produced from the neutral gas molecules by electron impact in the ionization region and then accelerated electrostatically down the ≈ 1-m-long ion flight tube to a micro-channel plate (MCP) detector. In the absence of electron impact induced fragmentation, the ionization process does not significantly alter the momentum of the molecule, so the molecular ions are born with the same transverse velocities as their parent molecules. We can compensate for these transverse velocities by "tuning" the voltage applied to a pair of ion deflection electrodes. This way, ions with a relatively narrow range of kinetic energies (instead of "velocities" for independence from the ion mass) can be steered onto the MCP detector.

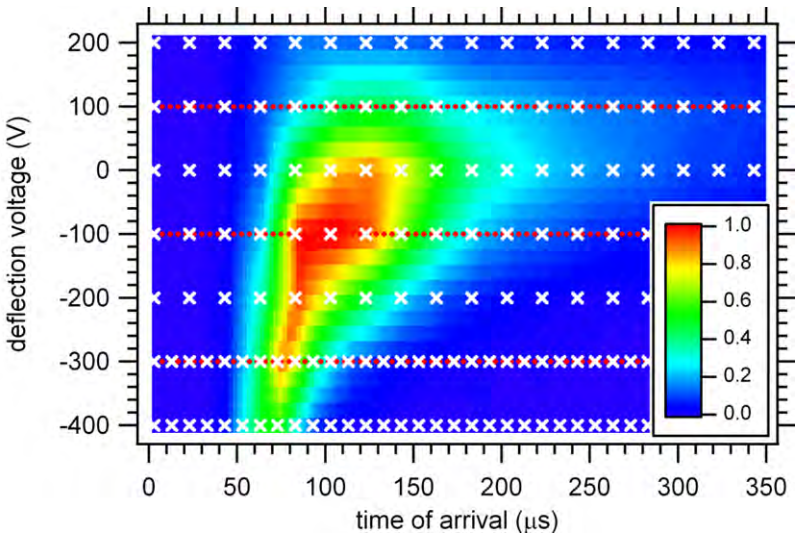


**Figure 44. $Al^+$ ion signal *vs.* Al atom arrival time and ion deflection voltage**
*Fast Al atoms produced by laser ablation of Al metal. [EF02145]*

Figure 44 shows our successful effort to detect hyperthermal Al atoms produced by laser ablation of Al metal [91]. The distance from the ablated sample spot to the TOFMS ionization region is 0.68 m, so a neutral time-of-arrival of 100 μs corresponds to an atomic Al velocity of 6.8 km/s and an atomic kinetic energy (KE) of 6.5 eV. Our approach to correcting and converting these raw data into the Al atom kinetic energy distribution shown in Figure 45 is discussed in great detail in ref. [91]. Briefly: we determined that if we measured the $Al^+$ signal on a dense mesh of Al atom arrival times and deflection voltages (the white Xs in Figure 44) we could then correct selected data for the velocity-dependent detection biases determined using SIMION [99] ion trajectory simulations, and then further transform them into neutral species velocity and kinetic energy distributions. Using this apparatus, we also reported preliminary TOFMS data of hyperthermal organic molecular species produced by direct laser ablation/ignition of thin-film nitrocellulose [91] and PETN [90] samples.

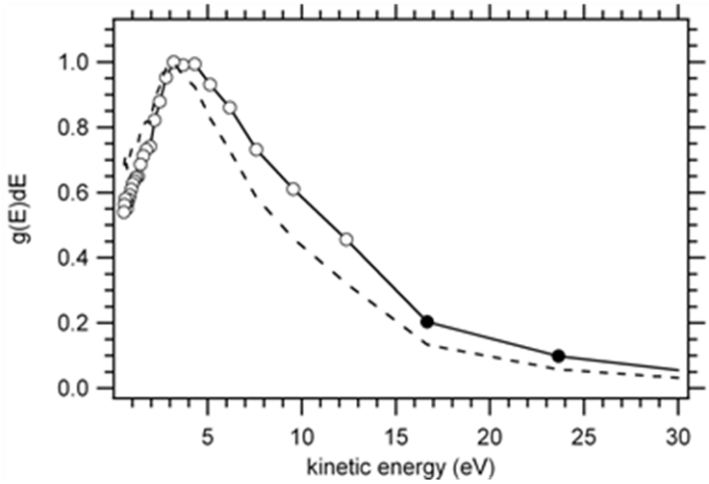


**Figure 45. Transformed & corrected Al atom kinetic energy distribution**

## 4. LESSONS LEARNED AND FUTURE DIRECTIONS

We end this report with a self-evaluation made with the benefit of hindsight, and some suggestions for ongoing and future efforts in this field.

### 4.A. Programmatic Lessons

The original rationale for this Project remains valid. While the scientific objectives have evolved, none of the work to date has disproved the basic premise of the utility of laboratory bench-scale experimentation on energetic materials. If anything, the field seems to be growing, as evidenced by presentations made by members of research groups from around the world at the American Physical Society Shock Compression of Condensed Matter meeting in July 2011. Our Benchtop Energetics effort is well-placed to participate in this field as a peer, demonstrated by our ongoing collaborations with researchers at Sandia National Laboratory (SNL), the Louisiana State University, and the University of Central Florida. The initial AFOSR investment in this project has produced a research team and laboratory facilities with unique capabilities that should remain viable and active under alternative funding for several years.

The original schedule was grossly overoptimistic. We underestimated the difficulties in: (1) setting up and permitting a new laboratory dedicated to novel experimental activities involving energetic materials, (2) procuring, integrating, and adapting our experimental apparatus within the constraints of our organizational support processes, and (3) attracting and retaining research personnel. We were also blissfully ignorant of the number and severity of *unknown* technical challenges that escaped un-noticed in the Proposal (more discussion below), and which eventually forced us to abandon certain approaches and make a number of major course corrections; such is basic research. With regard to the personnel issue, the lion's share of the progress during this project is due to the participation of team members (WKL, ECF, and CDM) brought in *via* the National Research Council (NRC) postdoctoral Research Associateship Program. AFOSR's support of this NRC program was arguably even more important to the Benchtop Energetics project than their direct funding.

### 4.B. Evolving Research Strategy

The emphasis in the Proposal on nanoenergetics was premature. Most practical energetic materials are composites with constituent particle sizes spanning microns to millimeters. It seemed absurd to propose shock initiation experiments on 10-μm-thick thin-film samples studded with 30-μm-diameter aluminum "boulders," so the use of nanometer scale ingredients provided a plausible route to on-the-average "homogeneous" composite samples. We should have realized that mitigating some of the risk in developing novel laboratory diagnostics would require more time initially spent working with simple single component energetic materials, such as pure PETN. As shown above in Figures 40 & 41, we did succeed in testing nanoenergetic materials early on with the 1$^{st}$ generation TOFMS apparatus, but the limitations of that instrument have precluded a definitive analysis of those data. We are actively pursuing experiments with nanoenergetic materials in the 2$^{nd}$ generation TOFMS apparatus, so while the schedule has slipped (considerably) the proposed work will be performed.

The opportunity to test fundamental detonation models proved irresistible. Re-reading the original motivation for the LANL DCA in ref. [97], in light of our new understanding gained from designing and analyzing the 2nd generation TOFMS apparatus, lead to a new insight: we have developed a novel apparatus that may be capable of producing qualitatively different data that could impact the fundamental understanding of detonation phenomena at very small scales. This notion is discussed in detail in ref. [91], and the argument is too long to reproduce here. However, if we eventually deliver on this promise, then this project will have made a far greater impact than was dreamt of during the proposal writing stage; such is basic research.

### 4.C. Evolving Research Tactics

The differential pumping approach used in the LANL DCA is truly necessary.

Time-of-flight mass spectrometry has proven more valuable than emission spectroscopy. Once the energetic material sample size becomes small enough that the physical danger to equipment and research personnel becomes negligible, the advantage of passive remote sensing enjoyed by the emission spectroscopy method becomes moot. Emission spectroscopy yields information only about those species cooperative enough to "glow" on demand and which are not buried deep within a dusty, opaque fireball. Thus, it is a far less general technique than the TOFMS approach since pretty much any molecule produces ions when hit by 70 eV electrons. We hope to revisit emission spectroscopy, and more sophisticated laser-based spectroscopies, in the future -- if we require the very specific information that these methods provide. Notably, one of us (WKL) has gone on to employ emission spectroscopy to determine the apparent temperatures of fireballs produced by ≈ 40 g explosive charges [100].

Direct laser initiation is a lot easier than shock initiation *via* laser driven flyers. We have invested much effort in learning to launch laser driven flyers, and in implementing our multiple-spot version of the very clever Buelow sample configuration discussed above in Section 3.E.1. However, we still have not made the key free-surface velocity measurements on the SS foil barriers necessary to estimate the shock loading of the overlying energetic material samples. Absent this information, we have resorted to the easy-to-implement laser-driven exploding foil initiation scheme mentioned as our fall-back position in Section 2.C of the Proposal. We used this approach in the energetic material experiments reported in refs. [90] & [91]. We hope to address this deficiency in the near future, and are working on a novel approach to making 2-dimensional velocity map measurements on the impacted SS foils.

The high-speed photographic diagnostic has been very valuable. Seeing visually where and when the energetic material is reacting has proven invaluable; for example, in understanding the source of the ≈ 3000 K blackbody flyer impact luminescence depicted in Figures 34-36. We have recently acquired a high-speed motion picture camera capable of recording at 1 million frames per second to complement our older single frame IgCCD camera.

Focused "top-hat" laser spots are easier to produce than we thought. Our interest in the relay-imaging approach arose from confusing the optical terms "to focus" and "to image." Once this was kindly explained to us by very helpful new friends [93], we implemented the single lens imaging scheme shown in Figure 11. The enlightenment was well worth the embarrassment.

Working in a buffer gas requires a gas circulation/filtration system. As discussed in Section 3.B, the persistent smoke that builds up in the chamber after launching a few flyers causes problems with dielectric breakdown in the laser beam prior to it reaching the sample. In the evacuated chamber, all the gases and particles produced by the laser travel in straight lines until they hit a chamber wall. The particles either stick where they hit, or else they fall to the bottom of the chamber. We periodically clean the chamber interior to prevent the buildup of appreciable amounts of solid energetic material residue.

Don't let a 1 km/s metal flyer impact directly on a viewport window. See Figure 15. We are presently concerned with preventing damage to the molecular beam forming skimmers from hypervelocity projectiles. This limits the thickness of the sacrificial metal foils we use in laser driven exploding foil initiation experiments to less than 1 μm.

Use a perforated mask to minimize flyer foil detachment and petalling. The individual circular holes in the mask also serve as a very short "gun barrels" to help extract additional work from the expanding laser plasma, further accelerating the flyers, as indicated in Figure 29.

Bubblegum and sticky tape can only take you so far. The quantity and quality of data produced from samples held together with MIL-T-23397B TYPE II aluminum tape is impressive; see, for example, Figure 27. The transition to sample coupons assembled on the SS frame and holder shown in Figure 20 was inevitable. This level of standardization is necessary to enable the use of energetic material samples produced by external collaborators. The major problem encountered with "sandwich" assemblies produced by stacking layers in the SS frame is an upward "bowing" of the centers of the layers. This bowing increases if the nuts pushing down on the captured spacers on each vertical alignment post are over-tightened. This is due to the absence of metal completely surrounding the base of each vertical alignment post, resulting in uneven support of the load imposed by tightening the nuts holding the assembly together. The next iteration will feature alignment posts surrounded by complete bearing surfaces.

Producing uniform energetic material spots is **much** more difficult than expected. Spin-coating produces nice films of polymeric materials, but not isolated spots. We had missed the literature on the "coffee ring stain" effect when we proposed the drop cast method for producing numerous isolated sample spots. Spray painting solutions with volatile organic solvents is a proven method for making sintered thin films, but poses serious safety issues for use with energetic materials (which we are addressing). These difficulties prompted the collaboration with researchers at SNL who are experts at physical vapor deposition (PVD) of explosives.

We should have specified a 1 or 2 Hz Nd:YAG laser pulse repetition rate. These lasers can only be operated at the repetition rate for which they are thermally compensated at the factory. We originally desired the 10 Hz repetition rate to minimize the time required to consume a sample coupon, but we are limited by slow data acquisition schemes to one event every few seconds. The other pulses are wasted, and represent unnecessary wear and tear on the flashlamps and other laser components. Indeed, we could accommodate the intrinsically slower repetition rates of a Nd:glass laser, if we required pulse energies above ≈ 3 J.

## REFERENCES


[1] H.E. Montgomery, Jr., U.S. Patent #3,961,576, "Reactive Fragment."

[2] Committee on Advanced Energetic Materials and Manufacturing Technologies, "Reactive Materials," Chapter 4 in Advanced Energetic Materials, (National Academies Press, Washington DC, 2004).

[3] S.C. Schmidt, D.P. Dandekar, and J.W. Forbes, eds., Shock Compression of Condensed Matter -- 1997, AIP Conference Proceedings 429, (AIP Press, New York, 1998).

[4] M.D Furnish, L.C. Chhabildas, and R.S. Hixson, eds., Shock Compression of Condensed Matter -- 1999, AIP Conference Proceedings 505, (AIP Press, New York, 2000).

[5] M.D Furnish, N.N. Thadhani, and Y. Horie, eds., Shock Compression of Condensed Matter -- 2001, AIP Conference Proceedings 620, (AIP Press, New York, 2002).

[6] Bulletin of the American Physical Society Vol. 48, No. 4 (2003). 13th APS Topical Conference on Shock Compression of Condensed Matter, held 20-25 July 2003 in Portland, OR.

[7] L.C. Yang and V.J. Menichelli, Appl. Phys. Lett. **19**, 473 (1971). "Detonation of Insensitive High Explosives by a Q-Switched Ruby Laser."

[8] R. Decoste, S.E. Bodner, B.H. Ripin, E.A. McLean, S.P. Obenschain, and C.M. Armstrong, Phys. Rev. Lett. **42**, 1673 (1979). "Ablative acceleration of laser-irradiated thin-foil targets."

[9] S.P. Obenschain, R.R. Whitlock, E.A. McLean, B.H. Ripin, R.H. Price, D.W. Phillion, E.M. Campbell, M.D. Rosen, and J.M. Auerbach, Phys. Rev. Lett. **50**, 44 (1983). "Uniform ablative acceleration of targets by laser irradiation at $10^{14}$ W/cm$^2$."

[10] D.L. Paisley, U.S. Patent # 5,046,423 (1991). "Laser-driven flyer plate."

[11] R. Fabbro, J. Fournier, P. Ballard, D. Devaux, and J. Virmont, J. Appl. Phys. **68**, 775 (1990). "Physical study of laser-produced plasma in confined geometry."

[12] D. Devaux, R. Fabbro, L. Tollier, and E. Bartnicki, J. Appl. Phys. **74**, 2268 (1993). Generation of shock waves by laser-induced plasma in confined geometry."

[13] R. Roybal, P. Tlomak, C. Stein, and H. Stokes, Int. J. Impact Eng. **23**, 811 (1999). "Simulated Space Debris Impact Experiments on Toughened Laminated Thin Solar Cell Cover Glass."

[14] D.B. Stahl, R.J. Gehr, R.W. Harper, T.D. Rupp, S.A. Sheffield, and D.L. Robbins, "Flyer velocity characteristics of the laser-driven Miniflyer system," p. 1087 in ref. [4].

[15] W.M. Trott, R.E. Setchell, and A.V. Farnsworth, Jr., "Investigation of the effects of target material strength on the efficiency of acceleration of thick laser driven flyers," p. 1203 in ref. [4].

[16] J.L. Labaste, D. Brisset, and M. Doucet, "Investigation of driving plasma materials for laser acceleration of flyer plates," p. 1189 in ref. [4].

[17] S. Watson and J.E. Field, J. Phys. D. Appl. Phys. **33**, 170 (2000). "Measurement of the ablated thickness of films in the launch of laser-driven flyer plates."

[18] K.A. Tanaka, M. Hara, N. Ozaki, Y. Sasatani, K. Kondo, M. Nakano, K. Nishihara, H. Takenaka, M. Yoshida, K. Mima, Phys. Plasmas **7**, 676 (2000).

"Multi-layer flyer accelerated by laser induced shock waves."
[19] S. Watson and J.E. Field, J. Appl. Phys. **88**, 3859 (2000).
"Integrity of thin, laser-driven flyer plates."
[20] S. Watson, M.J. Gifford, and J.E. Field, J. Appl. Phys. **88**, 65 (2000).
"The initiation of fine grain pentaerythritol tetranitrate by laser-driven flyer plates."
[21] M.W. Greenaway, M.J. Gifford, W.G. Proud, J.E. Field, and S.G. Goveas, "An investigation into the initiation of hexanitrostilbene by laser-driven flyer plates," p. 1035 in ref. [5].
[22] D.L. Paisley, D.C. Swift, R.P. Johnson, R.A. Kopp, and G.A. Kyrala, "Laser-launched flyer plates and direct laser shocks for dynamic material property measurements," p. 1343 in ref. [5].
[23] W.M. Trott, R.E. Setchell, and A.V. Farnsworth, Jr., "Development of laser-driven flyer techniques for equation-of-state studies of microscale materials," p. 1347 in ref. [5].
[24] A.V. Farnsworth, Jr., W.M. Trott, and R.E. Setchell, "A computational study of laser driven flyer plates," p. 1355 in ref. [5].
[25] J. Weston, Laser Focus World, May (1999).
"Relay imaging meets unique amplifier demands."
[26] R.M. Stevenson, M.J. Norman, T.H. Bett, D.A. Pepler, C.N. Danson, and I.N. Ross, Opt. Lett. **19**, 363 (1994). "Binary-phase zone plate arrays for the generation of uniform focal profiles."
[27] M. Koenig, B. Faral, J.M. Boudenne, D. Batani, A. Benuzzi, and S. Bossi, Phys. Rev. E **50**, R3314 (1994). Optical smoothing techniques for shock wave generation in laser produced plasmas."
[28] T. Lehecka, R.H. Lehmberg, A.V. Deniz, K.A. Gerber, S.P. Obenschain, C.J. Pawley, M.S. Pronko, and C.A. Sullivan, Opt. Comm. **117**, 485 (1995).
"Production of high energy, uniform focal profiles with the Nike laser."
[29] S.P. Chang, J.M. Kuo, Y.P. Lee, C.M. Lu, and K.J. Ling, Appl. Opt. **37**, 747 (1998).
"Transformation of Gaussian to coherent uniform beams by inverse-Gaussian transmittive filters."
[30] Q. Tan, Y. Yan, G. Jin, and M. Wu, Opt. Lasers Eng. **35**, 165 (2001). "Large aperture continuous phase diffractive optical element to realize uniform focal spot."
[31] M.W. Greenaway, W.G. Proud, J.E. Field, and S.G. Goveas, Rev. Sci. Instrum. **73**, 2185 (2002).
"The development and study of a fiber delivery system for beam shaping."
[32] B.R. Frieden, Appl. Opt. **4**, 1400 (1965).
"Lossless conversion of a plane laser wave to a plane wave of uniform irradiance."
[33] J.L. Kreuzer, U.S. Patent # 3,476,463 (1969). "Coherent light optical system yielding an output beam of desired intensity distribution at a desired equiphase surface."
[34] D. Shafer, Opt. Laser Technology, June (1982).
"Gaussian to flat-top intensity distributing lens."
[35] J.J. Kasinski and R.L. Burnham, Opt. Lett. **22**, 1062 (1997).
"Near-diffration-limited laser beam shaping with diamond-turned aspheric optics."
[36] J.A. Hoffnagle and C.M. Jefferson, Appl. Opt. **39**, 5488 (2000). "Design and performance of a refractive optical system that converts a Gaussian to a flattop beam."
[37] J.A. Hoffnagle and C.M. Jefferson, U.S. Patent # 6,295,168 (2001).
"Refractive optical system that converts a laser beam to a collimated flat-top beam."

[38] Y.B. Zeldovich and Y.P. Raizer, Physics of Shock Waves and High-Temperature Hydrodynamic Phenomena, W.D. Hayes and R.F. Probstein, eds., (Dover, Mineola, NY, 2002).
[39] S.P. Marsh, ed., LASL Shock Hugoniot Data, (U. California Press, Berkeley, CA, 1980).
[40] P.W. Cooper, Explosives Engineering, (Wiley-VCH, New York, NY, 1996).
[41] J.E. Kennedy and C.L. Mader, Applied Explosive Science, (Educational Technology Inc., San Diego, CA 2002).
[42] M. Boustie, C. Seymarc, E. Auroux, T. deResseguier, and J.P. Romain, "Coating debonding induced by confined laser shock interpreted in terms of shock wave propagation," p. 985 in ref. [3].
[43] L. Tollier, R. Fabbro, and E. Bartnicki, J. Appl. Phys. **83**, 1224 (1998). "Study of the laser-driven spallation process by the velocity interferometer system for any reflector interferometry technique. I. Laser-shock characterization."
[44] L. Tollier and R. Fabbro, J. Appl. Phys. **83**, 1231 (1998). "Study of the laser-driven spallation process by the velocity interferometer system for any reflector interferometry technique. II. Experiment and simulation of the spallation process."
[45] E. S. Hertel, Jr., R. L. Bell, M. G. Elrick, A. V. Farnsworth, G. I. Kerley, J. M. McGlaun, S. V. Petney, S. A. Silling, P. A. Taylor, and L. Yarrington, "CTH: A Software Family for Multi-Dimensional Shock Physics Analysis," in Proceedings of the 19th International Symposium on Shock Waves, Vol. I, R. Brun and L. D. Dumitrescu, eds., p377, Marseille, France 26-30 July 1993.
[46] L. Pasternack and J.K. Rice, J. Phys. Chem. **97**, 12805 (1993). "Laser ablation of $NH_4NO_3$."
[47] J.K. Rice and T.P. Russell, Chem. Phys. Lett. **234**, 195 (1995). "High-pressure matrix isolation of heterogeneous condensed phase chemical reactions under extreme conditions."
[48] T.P. Russell, T.M. Allen, and Y.M. Gupta, Chem. Phys. Lett. 267, 351 (1997). "Time resolved optical spectroscopy to examine chemical decomposition of energetic materials under static high pressure and pulsed heating conditions."
[49] L.J. Parker, H.D. Ladoceur, and T.P. Russell, "Teflon and Teflon/Al (nanocrystalline) decomposition chemistry at high pressures." p. 941 in ref. [4].
[50] A.B. Kunz, M.M. Kuklja, T.R. Botcher, and T.P. Russell, Thermochimica Acta **384**, 279 (2002). "Inititation of chemistry in molecular solids by processes involving electronic excited states."
[51] C.A. Wight and T.R. Botcher, J. Am. Chem. Soc. **114**, 8303 (1992). "Thermal decomposition of solid RDX begins with N-N bond scission."
[52] T.R. Botcher and C.A. Wight, J. Phys. Chem. **97**, 9149 (1993). "Transient thin film laser pyrolysis of RDX."
[53] T.R. Botcher and C.A. Wight, J. Phys. Chem. **98**, 5441 (1994). "Explosive thermal decomposition mechanism of RDX."
[54] I.Y.S. Lee, J.R. Hill, and D.D. Dlott, J. Appl. Phys. **75**, 4975 (1994). "Ultrafast microscopy of shock waves using a shock target array with an optical nanogauge."
[55] D.E. Hare, J. Franken, D.D. Dlott, E.L. Chronister, and J.J. Flores, Appl. Phys. Lett. **65**, 3051 (1994). "Dynamics of a polymer shock optical microgauge studied by picosecond coherent Raman spectroscopy."
[56] D.E. Hare, J. Franken, and D.D. Dlott, J, Appl. Phys. **77**, 5950 (1995).

"Coherent Raman measurements of polymer thin-film, pressure and temperature during picosecond laser ablation."
[57] D.E. Hare, J. Franken, and D.D. Dlott, Chem. Phys. Lett. **244**, 224 (1995). "A new method for studying picosecond dynamics of shocked solids: application to crystalline energetic materials."
[58] I.Y.S. Lee, J.R. Hill, H. Suzuki, D.D. Dlott, B.J. Baer, and E.L. Chronister, J. Chem. Phys. **103**, 8313 (1995). "Molecular dynamics observed 60 ps behind a solid-state shock front."
[59] S.A. Hambir, J. Franken, D.E. Hare, E.L. Chronister, B.J. Baer, and D.D. Dlott, J. Appl. Phys. **81**, 2157 (1997). "Ultrahigh time-resolution vibrational spectroscopy of shocked molecular solids."
[60] G. Tas, S.A. Hambir, J. Franken, D.E. Hare, and D.D. Dlott, J. Appl. Phys. **97**, 1080 (1997). "Coherent Raman spectroscopy of nanoshocks."
[61] D.D. Dlott, S. Hambir, and J. Franken, J. Phys. Chem. B **102**, 2121 (1998). "The new wave in shock waves."
[62] S. Wang, Y. Yang, Z. Sun, and D.D. Dlott, Chem. Phys. Lett. **368**, 189 (2003). "Fast spectroscopy of energy release in nanometric explosives."
[63] Y. Yang, Z. Sun, S. Wang, and D.D. Dlott, J. Phys. Chem. B **107**, 4485 (2003). "Fast Spectroscopy of laser-initiated nanoenergetic materials."
[64] E.S. Marmar, J.L. Cecchi, and S.A. Cohen, Rev. Sci. Instrum. **46**, 1149 (1975). "System for rapid injection of metal atoms into plasmas."
[65] J.H. Reho, D.S. Moore, D.J. Funk, G.L. Fisher, and R.L. Rabie, "Ultrafast spectroscopic investigation of shock cpmpressed glycidyl azide polymer and nitrocellulose films," p. 1219 in ref. [5].
[66] D.S. Moore, D.J. Funk, K.T. Gahagan, J.H. Reho, G.L. Fisher, S.D. McGrane, and R.L. Rabie, "Sub-picosecond laser-driven shocks in metals and energetic materials," p. 1333 in ref. [5].
[67] K.T. Gahagan, J.H. Reho, D.S. Moore, D.J. Funk, and R.L. Rabie, "Ultrafast time-resolved 2D spatial interferometry for shock wave characterization in metal films," p. 1351 in ref. [5].
[68] M.E. Fajardo, "Velocity selection of fast laser ablated metal atoms by a novel nonmechanical technique: temporally and spatialy specific photoionization (TASSPI)," PL-TR-97-3051 (Edwards AFB, CA 1998).
[69] G.I. Pangilinan and T.P. Russell, J. Chem. Phys. **111**, 445 (1999). "Role of Al-$O_2$ chemistry in the laser-induced vaporization of Al films in air."
[70] K. Wakabayashi, K.G. Nakamura, K. Kondo, and M. Yoshida, Appl. Phys. Lett. 75, 947 (1999). "Time-resolved Raman spectroscopy of polytetrafluoroethylene under laser-driven shock compression."
[71] K.G. Nakamura, K. Wakabayashi, and K. Kondo, "Transient bond scission of polytetrafluoroethylene under laser-driven shock compression studied by nanosecond time-resolved Raman spectroscopy."
[72] H. Nagao, A. Matsuda, K.G. Nakamura, and K.Kondo, Appl. Phys. Lett. 83, 249 (2003). "Nanosecond time resolved Raman spectroscopy on phase transition of polytetrafluoroethylene under laser-driven shock compression."
[73] M. Macler and M.E. Fajardo, Mat. Res. Soc. Symp. Proc. **285**, 105 (1993). "Determination of Atomic Velocity Distributions Using Transient Absorption

Measurements."
[74] G. Herzberg, Molecular Spectra and Molecular Structure Vol. I. Spectra of Diatomic Molecules, (Krieger, Malabar, FL 1989).
[75] http://www.dupont.com/teflon/chemical/pdf/h44587-3.pdf
[76] M.E. Fajardo and W.K. Lewis, "Progress Towards a Benchtop Energetics Capability." Poster presentation, AFOSR Molecular Dynamics and Theoretical Chemistry Contractors Meeting, Westin Arlington Gateway, Arlington, VA, 5-7 June 2006. AAC/PA 05-31-06-261.
[77] M.E. Fajardo and W.K. Lewis, "Progress Towards a Benchtop Energetics Capability." Invited oral presentation, 232nd American Chemical Society National Meeting, 10-14 September 2006, San Francisco, CA. AAC/PA 08-29-06-415.
[78] M.E. Fajardo and W.K. Lewis, "Benchtop Insensitivity: First Steps With PETN." Poster presentation, AFOSR Molecular Dynamics and Theoretical Chemistry Contractors Meeting, Beckman Center, Irvine, CA, 20-22 May 2007. AAC/PA 05-17-07-407.
[79] W.K. Lewis,V. Ashley, and M.E. Fajardo, "Big Influences from Small Particles: The Chemistry of Pentaerythritol Tetranitrate (PETN) Explosives Doped with Aluminum Nano-Particles." Invited oral presentation, Southeast Regional Meeting of the American Chemical Society, Greenville, SC, 23-27 October 2007. AAC/PA 10-15-07-604.
[80] M.E. Fajardo and W.K. Lewis, "Experimental Results from the 1st Generation Benchtop Energetics Apparatus." Oral presentation, AFOSR Molecular Dynamics and Theoretical Chemistry Contractors Meeting, Vienna, VA, 19-21 May 2008. 96th ABW/PA 04-30-08-243.
[81] M.E. Fajardo and W.K. Lewis, "Progress Towards a Benchtop Energetics Capability – First Steps With PETN." Invited oral presentation, Gordon Research Conference on Energetic Materials, Tilton School, Tilton, NH, 16 June 2008. 96th ABW/PA 04-30-08-243.
[82] C.D. Molek, R.M. Nep, E.C. Fossum, and M.E. Fajardo, "Benchtop Energetics Tool Sharpening." Poster presentation, AFOSR Molecular Dynamics Contractors Meeting, Chantilly, VA, 24-26 May 2010. 96ABW-2010-0283.
[83] E.C. Fossum, C.D. Molek, and M.E. Fajardo, "Benchtop Energetics – Mass Spectrometry of Fast Detonation Intermediates and Products. Poster presentation, AFOSR Molecular Dynamics Contractors Meeting, Chantilly, VA, 24-26 May 2010. 96ABW-2010-0289.
[84] C.D. Molek, R.M. Nep, E.C. Fossum, and M.E. Fajardo, "Benchtop Energetics Tool Sharpening." Poster presentation, Gordon Research Conference on Energetic Materials, Tilton School, Tilton, NH, 96ABW-2010-0357.
[85] E.C. Fossum, C.D. Molek, and M.E. Fajardo, "Benchtop Energetics – Mass Spectrometry of Fast Detonation Intermediates and Products. Poster presentation, Gordon Research Conference on Energetic Materials, Tilton School, Tilton, NH, 13-18 Jun 2010. 96ABW-2010-0358.
[86] M.E. Fajardo, "Benchtop Energetics Apparatus – Hyperthermal Species Detection via Time-Of-Flight Mass Spectrometry." Invited oral presentation, U. of West Florida, Department of Chemistry, Chemistry Seminar, 11 Febrary 2011, 96ABW-2011-0051.
[87] M.E. Fajardo, "Benchtop Energetics Progress." Invited oral presentation, 17th APS Topical Conference on Shock Compression of Condensed Matter, Chicago, IL, 27 Jun 2011. 96ABW-2011-0291. **(**AFRL-RW-EG-TP-2011-023)

[88] E.C. Fossum, "Benchtop Energetics – Detection of Hyperthermal Species." Oral presentation, 17th APS Topical Conference on Shock Compression of Condensed Matter, Chicago, IL, 27 Jun 2011. 96ABW-2011-0284.
[89] M.E. Fajardo, E.C. Fossum, C.D. Molek, and W.K. Lewis, AIP Conf. Proc. **vvvv**, ppp (2012). "Benchtop Energetics Progress."
[90] E.C. Fossum, C.D. Molek, W.K. Lewis, and M.E. Fajardo, AIP Conf. Proc. **vvvv**, ppp (2012). "Benchtop Energetics: Detection of Hyperthermal Species."
[91] E.C. Fossum, C.D. Molek, W.K. Lewis, and M.E. Fajardo, Propellants, Explosives, Pyrotechnics, accepted (2012). "Benchtop Energetics: Hyperthermal Species Detection."
[92] F. L. Pedrotti and L. S. Pedrotti, Introduction to Optics, (Prentice-Hall, Englewood Cliffs, NJ, 1987).
[93] S.D. McGrane and D.S. Moore, personal communication, 2010.
[94] R.D. Deegan, O. Bakajin, T.F. Dupont, G. Huber, S.R. Nagel, and T.A. Witten, Nature **389**, 827 (1997). "Capillary flow as the cause of ring stains from dried liquid drops."
[95] S.J. Buelow, J.E. Anderson, A.C. Aiken, C.A. Arrington Jr., and B. Jones, AIP Conf. Proc. **706**, 1377 (2003). "Mass Spectral Studies of Shocked Salts and Nitrocellulose Polymer Films."
[96] W.L. Ng, J.E. Field, and H.M., Hauser, J. Appl. Phys. **59**, 3945 (1986). "Thermal, fracture, and laser-induced decomposition of pentaerithritol tetranitrate,"
[97] N.C. Blais, H.A. Fry, N.R. Greiner, Rev. Sci. Instrum. **64**, 174 (1993). "Apparatus for the mass spectrometric analysis of detonation products quenched by adiabatic expansion."
[98] R. Engelke, N.C. Blais, and S.A. Sheffield, J. Phys. Chem. A **114**, 8234 (2010). "Mass-Spectroscopic Observations of Glycine Subjected to Strong Shock Loading."
[99] D.A. Dahl, Int. J. Mass Spectrom. **200**, 3 (2000). "SIMION for the personal computer in reflection."
[100] W.K. Lewis and C.G. Rumchik, J. Appl. Phys. **105**, 056104 (2009). "Measurement of apparent temperature in post-detonation fireballs using atomic emission spectroscopy."

DISTRIBUTION LIST
AFRL-RW-EG-TR-2012-009

*Defense Technical Info Center
8725 John J. Kingman Rd Ste 0944
Fort Belvoir VA 22060-6218

AFRL/RWME (6)
AFRL/RWOC-1 (STINFO Office)